If the light emission is coming from the bulk silicon, then the spectral distribution curve should be corrected for the self-absorption of the sample. The spectral distribution curve so corrected is indicated in Fig. 4.

If the light is identified with the avalanche breakdown process in the silicon, then two possible processes suggest themselves. The first process involves the radiative recombination of the high-energy electrons and holes produced in the junction region during breakdown. The radiation produced by this process would presumably have a low-energy threshold at about the band gap (~1 ev) of silicon. Since the probability of carriers having a given energy will decrease with increasing energy the spectral distribution would, of course, show a tailing off at the high-energy end as well.[5] The spectral distribution for this case might resemble the curve of Fig. 4. The results of Wolff's calculation[5] of the carrier distribution function would appear consistent with the observed spectral distribution curve. It would be expected that the light output would increase as the square of the current for this mechanism.

The second process involves an intraband relaxation That is, a high-energy carrier could lose its energy by radiation and drop into a lower level in its own band. Such a process would also produce a tailing off of the emission at high energies (see the foregoing). However, the radiation would presumably, not have a definite low-energy limit. It would be expected that the total light emission would be linear in current.

For both these radiation mechanisms the decay time for light emission would presumably be of order 0.1–0.01 μsec.[2] Our measurement indicated a decay time that was 4 μsec or less. This result was limited by the instrumentation.

In summary, the evidence suggests that the light emission results from radiative relaxation processes involving high-energy carriers in or near the barrier during avalanche breakdown. However, further study will be required before this conclusion can be made rigorous and a detailed mechanism elucidated.

[5] P. Wolff, Phys. Rev. **95**, 1415 (1954).

ACKNOWLEDGMENTS

I am indebted to R. N. Hall for bringing this problem to my attention. I should like to thank W. C. Dash for his help at various stages of the project. E. O. Kane suggested the intraband relaxation mechanism and was very helpful in discussing various phases of this work. I am also indebted to K. G. McKay for his comments on this manuscript.

PHYSICAL REVIEW VOLUME 100, NUMBER 2 OCTOBER 15, 1955

Stark Effect in Rapidly Varying Fields*

S. H. Autler† and C. H. Townes
Columbia University, New York, New York

(Received May 31, 1955)

A method is developed for calculating the effects of a strong oscillating field on two states of a quantum-mechanical system which are connected by a matrix element of the field. Explicit approximate solutions are obtained for a variety of special cases, and the results of numerical computations are given for others. The effect of an rf field on the $J=2\rightarrow1$ l-type doublet microwave absorption lines of OCS has been studied in particular both experimentally and theoretically. Each line was observed to split into two components when the frequency of the rf field was near 12.78 Mc or 38.28 Mc, which are the frequencies separating the $J=1$ and $J=2$ pairs of levels, respectively. By measuring the rf frequency, ν_0, at which the microwave lines are split into two equally intense components, one may determine the separation between the energy levels. The measured value of ν_0 depends upon the intensity of the rf field and the form of this dependence has been calculated and found to be in good agreement with the experimental results.

I. INTRODUCTION

1.1 Outline of the Problem

A RELATIVELY weak perturbation varying sinusoidally in time may affect a physical system by causing an occasional transition between quantum states. These transitions are accompanied by the absorption or emission of photons and may be observed spectroscopically. However, if the perturbation is strong enough, transitions are rapidly induced and a variety of other observable phenomena can occur. We shall discuss some of these in the case of a system where relaxation processes are negligible, i.e., where the effects of the sinusoidal perturbation are much more important than those due to processes which dissipate energy. In particular, an experiment will be described which involves the simultaneous effects of two electromagnetic fields on the molecules of gaseous OCS. One field is much stronger than the other and is in the radio-frequency range; the weaker field is in the microwave

* Work supported jointly by the Department of the Army (Signal Corps), the Department of the Navy (Office of Naval Research), and the Department of the Air Force (Air Research and Development Command).

† Present address: Lincoln Laboratory, Massachusetts Institute of Technology, Lexington, Massachusetts.

region and is transmitted through a wave guide containing the gas while absorption lines are observed by the usual techniques of microwave spectroscopy. At certain frequencies the rf field induces rapid transitions between the molecular states, which affects the absorption of the microwaves. The absorption of the rf field, which is not directly observable can thus be indirectly studied by microwave spectroscopy.

After a statement of definitions and a short introductory theory, some of the previously published work related to our subject is discussed. Then a general treatment is developed for the effects of a sinusoidally varying field of any strength and frequency on a simple quantum-mechanical system for which only two stationary states need be considered. The general solution is expressed in terms of infinite continued fractions, but simple approximations are given which are valid over certain ranges of field strength and frequency; for other ranges numerical results are given.

The case of "resonant modulation" where the frequency of the field coincides with an internal frequency of the system is of particular interest. Although our theoretical treatment was developed primarily for this case, and is compared in some detail with experimental results, it is applicable to a wider range of conditions including some found in molecular beam experiments.

1.2 Preliminary Theory and Definitions

The discussion of the effects of an oscillating field will be simplified by assuming that the wave function of the system may be expressed as a linear combination of just two of its unperturbed eigenfunctions. Thus,

$$\Psi = T_a(t)U_a + T_b(t)U_b, \tag{1}$$

where U_a and U_b are the space-dependent parts of these two eigenfunctions. The states are assumed to be nondegenerate and to have energies W_a and W_b with $W_b > W_a$. Relaxation processes will be completely ignored, so the energy levels are treated as perfectly sharp.

We may expect Eq. (1) to be a valid approximation in a number of cases. If the frequency of the perturbing field is close to $(W_b - W_a)/h$, it has a much greater effect on these two states than on others, which may then be ignored. This is also permissible for any frequency if W_a and W_b are much closer to each other than to any other states; this requirement is satisfied by the states of the OCS molecule which were studied in our experiment. Later a microwave field will be allowed to induce occasional transitions to a third state well removed in energy, but if this field is weak it has a relatively small effect on the states under study.

The time-dependent wave equation is

$$i\hbar\dot{\Psi} = [H^0 - \mathfrak{y}\cdot\mathbf{E}\cos\omega t]\Psi, \tag{2}$$

where H^0 = unperturbed Hamiltonian containing all internal interactions, $\mathfrak{y}$ = permanent electric dipole moment of molecule, $\mathbf{E}\cos\omega t$ = applied electric field. Substituting (1) into (2) gives

$$\begin{aligned} i\hbar\dot{T}_a &= W_aT_a + 2\hbar\beta_{ab}\cos\omega t T_b, \\ i\hbar\dot{T}_b &= W_bT_b + 2\hbar\beta_{ba}\cos\omega t T_a, \end{aligned} \tag{3}$$

where

$$\beta_{ab} = \frac{\langle a|\,\mathfrak{y}\cdot\mathbf{E}\,|b\rangle}{2\hbar}, \quad \beta_{ab} = \beta_{ba}$$

$$H^0U_a = W_aU_a, \quad H^0U_b = W_bU_b.$$

β_{aa} and β_{bb} equal zero if states a and b are nondegenerate. β_{ab} may be assumed real without loss of generality as any phase factor may be absorbed into T_a and T_b.

In spite of their rather simple appearance, these equations have not been solved in terms of tabulated functions. The complicated form of the equation

$$0 = \frac{\partial^2 T_a}{\partial t^2} + \left[\frac{i}{\hbar}(W_a + W_b) + \omega\tan\omega t\right]\frac{\partial T_a}{\partial t} + \left[4\beta_{ab}^2\cos^2\omega t - \frac{W_aW_b}{\hbar^2} + \frac{iW_a}{\hbar}\omega\tan\omega t\right]T_a$$

obtained by eliminating T_b from (3) indicates why this is so. One must therefore obtain approximate solutions for various values of the parameters β_{ab} and ω.

The ranges of β_{ab} and ω will be denoted as follows:

Field strength		Frequency	
Weak:	$\beta_{ab} \ll \omega_{ab}$	Low:	$\omega \ll \omega_{ab}$
Intermediate:	$\beta_{ab} \approx \omega_{ab}$	Resonant:	$\omega \approx \omega_{ab}$
Strong:	$\beta_{ab} \gg \omega_{ab}$	High:	$\omega \gg \omega_{ab}$

$$\omega_{ab} = (W_b - W_a)/h.$$

II. REVIEW OF RELATED WORK

2.1 Resonant Modulation

The authors have previously reported results of an experiment[1] in which a radio-frequency field was used to produce transitions between two energy levels of the molecules of OCS gas and thus modulate the probability of finding a molecule in either state. The gas was kept in a wave guide and a microwave absorption line involving one of the levels was observed while the rf field was applied across the wave guide. When the frequency of the rf field was made resonant with the separation between the two levels, the microwave absorption line appeared to split into two components of nearly equal intensity. Although the possibility of measuring energy differences by this method was established, there were certain discrepancies between observations and theory. In this paper, more precise experimental data and more detailed theory are reported and better agreement is obtained.

Time-dependent perturbation calculations are carried into a somewhat broader range of frequencies and field

[1] S. H. Autler and C. H. Townes, Columbia Radiation Laboratory Reports, June 30, 1949 and September 30, 1949 (unpublished). S. H. Autler and C. H. Townes, Phys. Rev. **78**, 340 (1950).

strengths in this paper than has previously been reported. Some previous results are reviewed below in order to show their relationship to the present work.

2.2 Extremely Weak Fields

In discussing the effect of a resonant field in inducing transitions between two stationary states, it may be assumed that the system is originally known to be in one of these states and that the probability of finding it in the other state remains small.[2] This gives a transition probability which increases as t^2. It is then usually assumed that the final state can be any one of a very closely spaced group of states, or that the radiation consists of a band of frequencies. This leads to the familiar result in which the transition probability grows linearly in time at a rate proportional to the square of the field strength until a collision or some other relaxation mechanism terminates the process.

2.3 Rotating Fields

For fields which are somewhat stronger, though still weak according to the definition adopted above, it is no longer possible to neglect the probability of finding the system in the second state. This problem has been discussed by Majorana and by Rabi[3] for the case of a magnetic dipole in a rotating magnetic field. For a spin of $\frac{1}{2}$, Rabi obtained the equations

$$\begin{aligned} i\hbar\dot{C}_{+\frac{1}{2}} &= \frac{g\mu_0 H_z}{2} C_{+\frac{1}{2}} + \frac{g\mu_0 H_\perp}{2} e^{-i\omega t} C_{-\frac{1}{2}}, \\ i\hbar\dot{C}_{-\frac{1}{2}} &= -\frac{g\mu_0 H_z}{2} C_{-\frac{1}{2}} + \frac{g\mu_0 H_\perp}{2} e^{+i\omega t} C_{+\frac{1}{2}}, \end{aligned} \tag{4}$$

where $H_\perp$ = component of rotating field which lies $\perp$ to H_z, H_z = average value of magnetic field $\mathbf{H}$, g = Landé g-factor of particle, μ_0 = Bohr magneton. $C_{+\frac{1}{2}}$ and $C_{-\frac{1}{2}}$ are the probability amplitudes of the two spin orientations.

The form of these equations differs from that of Eqs. (3) only in the replacement of $\cos\omega t$ by exponentials. This difference, however, allows Eqs. (4) to be solved exactly.

The result obtained is that the probability of finding the dipole in the $-\frac{1}{2}$ state, assuming it starts in the $+\frac{1}{2}$ state, is:

$$P(\tfrac{1}{2}, -\tfrac{1}{2}) = \frac{(g\mu_0 H_\perp)^2}{\hbar^2(\omega-\omega_0)^2 + (g\mu_0 H_\perp)^2} \times \sin^2\left\{\frac{t}{2}\left[(\omega-\omega_0)^2 + \left(\frac{g\mu_0 H_\perp}{\hbar}\right)^2\right]^{\frac{1}{2}}\right\}, \tag{5}$$

where $\omega_0 = g\mu_0 H_z/\hbar$ is the Larmor angular frequency of the dipole in the field.

The particle oscillates sinusoidally between the two states with an amplitude which is equal to one when $\omega = \omega_0$.

[2] L. Schiff, *Quantum Mechanics* (McGraw-Hill Book Company, Inc., New York, 1949), Chap. X.
[3] I. I. Rabi, Phys. Rev. **51**, 652 (1932).

Torrey[4] calculated this in a somewhat different manner in connection with an investigation of the line shape of molecular beam radio-frequency resonances. We shall use an approach similar to Torrey's, whose result is obtained as the first approximate solution of our general equations in Sec. 3.3.

2.4 Weak Oscillating Field

Equation (5), which describes precisely the effect of any rotating field, is also a good approximation for an oscillating field if that field is weak and its frequency near resonance. This is to be expected since a field varying as $\cos\omega t$ can be separated into two rotating fields, $\frac{1}{2}e^{+i\omega t}$ and $\frac{1}{2}e^{-i\omega t}$. One of these can be thought of as rotating with the precessing particle and the other oppositely. A small oppositely rotating field will have little effect compared to the resonant one. Bloch and Siegert[5] made an approximate calculation of this effect for the case of a particle of spin $\frac{1}{2}$ in a polarizing magnetic field by expressing the equivalent of Eq. (3) as an integral equation which was then expanded in a series. They showed that the first effect of the counter-rotating field is to increase the resonant frequency by the fractional amount $\frac{1}{16}(H_\perp/H_z)^2$. In our notation this can then be written

$$\omega_0/\omega_{ab} = 1 + (\beta_{ab}^2/\omega_{ab}^2),$$

where ω_0 is the observed resonant frequency. This result is discussed in Sec. 4.2.

2.5 Double Modulation

The simultaneous use of radio-frequency and ultraviolet radiation to investigate the structure of atomic energy levels has been described by Brossel, Kastler, and Bitter.[6] After exciting mercury vapor atoms by resonance radiation, they ingeniously employ the rf field to alter the population of the atoms in the excited state and then observe the change in polarization of the spontaneously emitted ultraviolet radiation. They obtained a radio-frequency resonance and splitting similar to that described in Sec. 2.1. The theory given for "resonant modulation" [1] is in fact applicable to Brossel and Bitter's case. However, Pryce[7] has independently calculated the splitting which occurs in this experiment. Brossel and Bitter also obtain a shift in the resonance approximately equal to that calculated by Bloch and Siegert.[5]

2.6 Low-Frequency Perturbation

If the frequency of the applied field is sufficiently low, its effect can be treated quasi-statically, i.e., the solution can be regarded at any instant as being the steady-state solution appropriate for the instantaneous field. The instantaneous value of the field appears as a parameter in the solution, and as the field varies, the solution is presumed to follow along.

[4] H. C. Torrey, Phys. Rev. **59**, 293 (1941).
[5] F. Bloch and A. Siegert, Phys. Rev. **57**, 522 (1940).
[6] J. Brossel and A. Kastler, Compt. rend. **229**, 1213 (1949); J. Brossel and F. Bitter, Phys. Rev. **86**, 308 (1952).
[7] M. H. L. Pryce, Phys. Rev. **77**, 136 (1950).

Townes and Merritt[8] calculated and observed the second-order Stark effect due to fields of several hundred kilocycles, and also calculated the first order case. They found that when ω is larger than the width of the absorption line each Stark component breaks up into lines spaced by the angular frequency ω, with amplitudes depending upon the field strength. In second-order Stark effect each energy level breaks up into a number of components with angular frequencies displaced from its unperturbed value by $\frac{1}{2}aE^2\pm 2n\omega$, where n is any integer, a is a constant, and E the field strength. Relative intensities of the components are given by $J_n^2(aE^2/2)$. The agreement between theory and experiment was found to be excellent. A derivation of the above result is given in Sec. 3.5.

Since the present work ignores the effects of collisions, the case where ω is comparable to the line width requires another treatment. This has been given by Karplus,[9] who used the methods of quantum statistics and treated in detail several cases where the molecular resonances are shifted by fields with particular wave forms.

III. THEORY

3.1 General Formulas

A solution is desired for T_a and T_b in Eq. (3). Use will be made of Floquet's theorem[10] which shows that T_a and T_b have the form

$$T_a=e^{i\lambda t}\sum_{n=-\infty}^{+\infty}A_ne^{-in\omega t},\quad T_b=e^{i\lambda t}\sum_{n=-\infty}^{+\infty}B_ne^{-in\omega t},\tag{6}$$

where n is any positive or negative integer or zero. If (6) is substituted into (3) after expressing $\cos\omega t$ in exponentials, and terms with the same exponents are equated, one obtains

$$\begin{aligned}(\lambda+\omega_a-n\omega)A_n&=-\beta_{ab}B_{n-1}-\beta_{ab}B_{n+1},\\(\lambda+\omega_b-n\omega)B_n&=-\beta_{ab}A_{n-1}-\beta_{ab}A_{n+1},\end{aligned}\tag{7}$$

where $\omega_a=W_a/\hbar$, $\omega_b=W_b/\hbar$. This set of equations can be separated into two completely independent sets as follows:

$$\begin{aligned}[L_a-k\omega/\beta_{ab}]A_k&=-B_{k-1}-B_{k+1},\\[L_a+\omega_{ab}/\beta_{ab}-l\omega/\beta_{ab}]B_l&=-A_{l-1}-A_{l+1},\end{aligned}\tag{8}$$

with all odd A's and even B's being zero. Also

$$\begin{aligned}[L_b-\omega_{ab}/\beta_{ab}-l\omega/\beta_{ab}]A_l&=-B_{l-1}-B_{l+1},\\[L_b-k\omega/\beta_{ab}]B_k&=-A_{k-1}-A_{k+1},\end{aligned}\tag{9}$$

with all odd B's and even A's equal to zero. Here

$$L_a\equiv\frac{\lambda+\omega_a}{\beta_{ab}},\quad L_b\equiv\frac{\lambda+\omega_b}{\beta_{ab}},$$

and k runs through all positive and negative even integers and zero; l runs through all positive and negative odd integers.

Since Eqs. (8) and (9) are independent, a complete solution may be obtained by adding any solution of (8) to any solution of (9).

We will first concentrate on (8), an infinite set of linear homogeneous equations with an infinite number of unknown quantities (the A's, B's, and λ) to be determined. One could set up the infinite secular determinant of the coefficients and attempt to solve it. Instead, the method to be used here is to express the ratios of the A's and B's as infinite continued fractions and then obtain an equation for λ involving them. This method of attack arises naturally and the continued fraction expressions are fairly amenable to algebraic and numerical calculations to any accuracy.

In Appendix 3.1a, it is shown that if one assumes that the amplitude coefficients (A's and B's) become negligible for $|k|$ and $|l|$ sufficiently large, then

$$\frac{A_{\pm k}}{B_{\pm(k-1)}}=\cfrac{-1}{L_a\mp k\frac{\omega_{ab}}{\beta_{ab}}\left(\frac{\omega}{\omega_{ab}}\right)-\cfrac{1}{L_a+\frac{\omega_{ab}}{\beta_{ab}}\mp(k+1)\frac{\omega_{ab}}{\beta_{ab}}\left(\frac{\omega}{\omega_{ab}}\right)-\cfrac{1}{L_a\mp(k+2)\frac{\omega_{ab}}{\beta_{ab}}\left(\frac{\omega}{\omega_{ab}}\right)-\cfrac{1}{L_a+\frac{\omega_{ab}}{\beta_{ab}}\mp(k+3)\frac{\omega_{ab}}{\beta_{ab}}\left(\frac{\omega}{\omega_{ab}}\right)-\cdots}}}},$$

$$\frac{B_{\pm l}}{A_{\pm(l-1)}}=\cfrac{-1}{L_a+\frac{\omega_{ab}}{\beta_{ab}}\mp l\frac{\omega_{ab}}{\beta_{ab}}\left(\frac{\omega}{\omega_{ab}}\right)-\cfrac{1}{L_a\mp(l+1)\frac{\omega_{ab}}{\beta_{ab}}\left(\frac{\omega}{\omega_{ab}}\right)-\cfrac{1}{L_a+\frac{\omega_{ab}}{\beta_{ab}}\mp(l+2)\frac{\omega_{ab}}{\beta_{ab}}\left(\frac{\omega}{\omega_{ab}}\right)-\cfrac{1}{L_a\mp(l+3)\frac{\omega_{ab}}{\beta_{ab}}\left(\frac{\omega}{\omega_{ab}}\right)-\cdots}}}}.\tag{10}$$

[8] C. H. Townes and F. R. Merritt, Phys. Rev. **72**, 1266 (1947).
[9] R. Karplus, Phys. Rev. **73**, 1027 (1948).
[10] H. Margenau and G. M. Murphy, *Mathematics of Physics and Chemistry* (D. Van Nostrand Company, Inc., New York, 1947), p. 80.

In reading the above expressions, either the upper or lower sign should be used throughout.

In Eq. (10), the ratios of successive amplitude coefficients are expressed as functions of ω_{ab}/β_{ab} and ω/ω_{ab}, two dimensionless quantities which are natural measures of the intensity and frequency of the applied field and completely determine the problem. L_a is defined as $(\lambda+\omega_a)/\beta_{ab}$ and in Eq. (11) below is given as a function of ω_{ab}/β_{ab} and ω/ω_{ab}. Equations (10) then may be regarded as expressing successive amplitude coefficients (A's and B's) as functions of the physical variables. For example, by letting l equal one, an expression for B_{+1}/A_0 is obtained. Similarly, $A_{\pm 2}/B_{\pm 1}$, $B_{\pm 3}/A_{\pm 2}$, etc., can all be expressed as continued fractions, and the ratio of any of the A's and B's to A_0 written as a product of these quantities. A_0 is one of the arbitrary constants which appear in a general solution of a second order differential equation, and may be evaluated by applying normalization and initial conditions to ψ.

Besides being necessary for calculating the amplitude coefficients, L_a has a physical interpretation which will be discussed at the end of Sec. 3.3.

By setting $k=0$ in Eq. (8) and then making use of Eq. (10), we obtain

$$L_a=\cfrac{1}{L_a+\cfrac{\omega_{ab}}{\beta_{ab}}\left(1-\cfrac{\omega}{\omega_{ab}}\right)-\cfrac{1}{L_a-2\left(\cfrac{\omega_{ab}}{\beta_{ab}}\right)\left(\cfrac{\omega}{\omega_{ab}}\right)-\cfrac{1}{L_a+\cfrac{\omega_{ab}}{\beta_{ab}}\left(1-\cfrac{3\omega}{\beta_{ab}}\right)-\cdots}}}+\cfrac{1}{L_a+\cfrac{\omega_{ab}}{\beta_{ab}}\left(1+\cfrac{\omega}{\omega_{ab}}\right)-\cfrac{1}{L_a+2\left(\cfrac{\omega_{ab}}{\beta_{ab}}\right)\left(\cfrac{\omega}{\omega_{ab}}\right)-\cdots}} \tag{11}$$

Equations (10) and (11) are general expressions which, at least in principle, can be used to determine L_a and then the amplitudes for all values of ω_{ab}/β_{ab} and ω/ω_{ab}. To actually solve (11) for L_a, one must in general retain only a finite number of the quotients in each continued fraction, but by retaining a sufficient number L_a can be evaluated to any desired accuracy. Eventually, the denominators are dominated by the terms of the form $n\omega/\beta_{ab}$ and the quotients approach zero; which is a necessary condition of the fractions are to converge. The larger ω/β_{ab}, the more rapid the convergence, so it will be necessary to retain fewer quotients for high frequencies and weak fields.

No proof has been obtained that the continued fractions always converge. However, it is shown in the Appendix 3.1b that when $\omega=0$, assuming convergence leads to the correct steady-state solution. That this is so in the case when one expects least rapid convergence indicates that the fractions probably converge in all other cases.

If only a few quotients need to be retained, Eq. (11) can be expressed as an algebraic equation of low degree and solved either exactly or approximately by familiar methods. This will be done for weak fields. For stronger fields where more quotients must be kept, it is easier to work numerically with the continued fractions themselves, and solutions for L_a have been obtained numerically for a wide range of frequencies and for fairly strong fields.

The equation obtained by retaining all terms and expressing Eq. (11) in powers of L_a, would be of infinite degree and have an infinite number of solutions. Fortunately, because of the periodic properties of the original differential equation, all these solutions are related in a simple manner, so that if one is known all the others may be readily obtained. In Appendix 3.1c, the following relations are proved:

Assume L_a, A_0, A_2, $\cdots$, B_1, B_3, $\cdots$ satisfy Eqs. (8). Then L_a', A_0', A_2', $\cdots B_1'$, B_3', $\cdots$ give another solution if

$$L_a'=-L_a-\frac{\omega_{ab}-(2m+1)\omega}{\beta_{ab}}, \tag{12}$$

and

$$B_l'=A_{2m+1-l}, \quad A_k'=-B_{2m+1-k}, \tag{13}$$

where m is any positive or negative integer.

Another set of solutions of (8) is

$$L_a''=L_a+2m(\omega/\beta_{ab}), \qquad A_k''=A_{k-2m}, \quad B_l''=B_{l-2m}. \tag{14}$$

There are other solutions which satisfy (9) rather than (8). In Appendix 3.1c, the following simple relationship between the solutions of (8) and (9) is proved: If L_a, $A_k/A_0\cdots$, $B_l/A_0\cdots$ define any solution of (8), then L_b, $A_l/B_0\cdots$, $B_k/B_0\cdots$ define a solution of (9), if

$$L_b=-L_a;\ A_l/B_0=-B_{-l}/A_0,\ B_k/B_0=+A_{-k}/A_0. \tag{15}$$

The solutions of (8) contain only even A's and odd B's while the reverse is true for (9).

A complete solution is obtained by adding any solution of (8) to any solution of (9). It is quite arbitrary which of the infinite number of solutions is used in each case, for they all contain the same physical information; the various solutions corresponding essentially to a relabeling of the amplitude coefficients. However, it is necessary to understand the nature of the solutions when actually making calculations to avoid errors which might arise by skipping from one solution to another without knowing it.

A complete solution is obtained by combining Eqs. (1) and (6).

$$\psi \equiv U_a\Big\{A_0 e^{i\lambda_a t}\sum_{\substack{k=-\infty\\ \text{even}}}^{+\infty}\frac{A_k}{A_0}e^{-ik\omega t} + B_0 e^{i\lambda_b t}\sum_{\substack{l=-\infty\\ \text{odd}}}^{+\infty}\frac{A_l}{B_0}e^{-il\omega t}\Big\} + U_b\Big\{A_0 e^{i\lambda_a t}\sum_{\substack{l=-\infty\\ \text{odd}}}^{+\infty}\frac{B_l}{A_0}e^{-il\omega t} + B_0 e^{i\lambda_b t}\sum_{\substack{k=-\infty\\ \text{even}}}^{+\infty}\frac{B_k}{B_0}e^{-ik\omega t}\Big\}. \quad (16)$$

Here λ_a, $A_k\cdots$, $B\cdots$ may form any solution of (8). λ_a is equal to $\beta_{ab}L_a-\omega_a$, where L_a is any solution of (11). Also

$$\frac{A_{\pm k}}{A_0}=\frac{A_{\pm k}}{B_{\pm(k-1)}}\cdot\frac{B_{\pm(k-1)}}{A_{\pm(k-2)}}\cdots\frac{B_{\pm 1}}{A_0};$$

$$\frac{B_{\pm l}}{A_0}=\frac{B_{\pm l}}{A_{\pm(l-1)}}\cdot\frac{A_{\pm(l-1)}}{B_{\pm(l-2)}}\cdots\frac{B_{\pm 1}}{A_0};$$

where the factors of the form $A_{\pm k}/B_{\pm(k-1)}$ and $B_{\pm l}/A_{\pm(l-1)}$ are expressed as continued fractions by (10). Similarly, λ_b, $A_l\cdots$, $B_k\cdots$ form a solution of (9).

The number of independent quantities in Eq. (16) may be reduced by first choosing a solution for L_a and then using (15) to derive the solution of (9) to be used. Define

$$\lambda_a=\beta_{ab}L_a-\omega_a, \quad \lambda_b=\beta_{ab}L_b-\omega_b,$$

and set

$$L_b=-L_a.$$

Then

$$\lambda_b=-\lambda_a-\omega_a-\omega_b.$$

Also,

$$\frac{A_l}{B_0}=-\frac{B_{-l}}{A_0}, \quad \frac{B_k}{B_0}=+\frac{A_{-k}}{A_0}.$$

Equation (16) can then be written

$$\psi = U_a e^{-\frac{1}{2}i(\omega_a+\omega_b)t}\Big\{|A_0|e^{i[\frac{1}{2}(\omega_a+\omega_b)+\lambda_a]t}\sum_{\substack{k=-\infty\\ \text{even}}}^{+\infty}\frac{A_k}{A_0}e^{-ik\omega t} - |B_0|e^{-i[\frac{1}{2}(\omega_a+\omega_b)+\lambda_a]t-i\theta}\sum_{\substack{l=-\infty\\ \text{odd}}}^{+\infty}\frac{B_l}{A_0}e^{+il\omega t}\Big\} - U_b e^{-\frac{1}{2}i(\omega_a+\omega_b)t}\Big\{|A_0|e^{i[\frac{1}{2}(\omega_a+\omega_b)+\lambda_a]t}\sum_{l=-\infty}^{+\infty}\frac{B_l}{A_0}e^{-il\omega t} + |B_0|e^{-i[\frac{1}{2}(\omega_a+\omega_b)+\lambda_a]t-i\theta}\sum_{k=-\infty}^{+\infty}\frac{A_k}{A_0}e^{ik\omega t}\Big\}, \quad (17)$$

where

$$e^{i\theta}\equiv\frac{B_0}{|B_0|}\Big/\frac{A_0}{|A_0|}$$

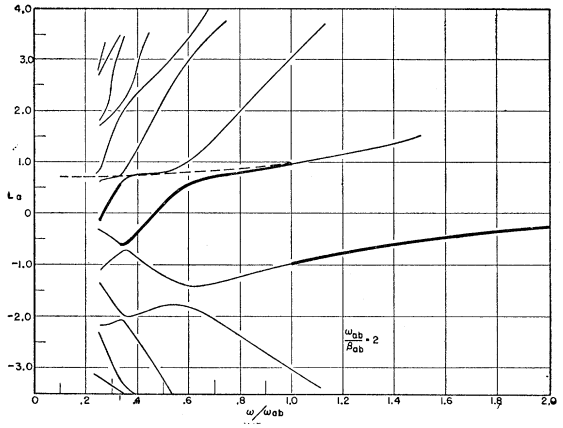

(a) Strong applied field, $\omega_{ab}/\beta_{ab}=2$.

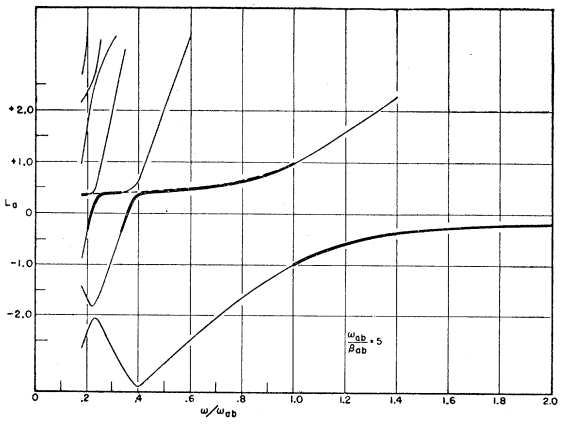

(b) Weaker applied field, $\omega_{ab}/\beta_{ab}=5$.

FIG. 1. The numerically computed solutions of Eq. (11) for L_a as a function of the frequency of the applied field. The darkened curves show the preferred solution in each range of ω/ω_{ab}. The dashed curves are plots of the approximation for L_a given by Eq. (33)

depends upon the relative phase of A_0 and B_0. A_0 and B_0 must be chosen so as to normalize ψ and satisfy the initial conditions. λ_a, $A_k/A_0\cdots$, $B_l/B_0\cdots$ may still form any one of the possible solutions of (8) and the particular one chosen is chiefly a matter of convenience.

In Fig. 1 the solutions of L_a are plotted as a function of the frequency for a number of field strengths. It is based on numerical computations which are discussed at the end of Sec. 3.3.

Although any of the possible solutions for L_a could be used in Eqs. (10) and (17) to give a consistent result, one choice is most natural. This is the solution which remains finite when the field intensity and, therefore, β_{ab} approaches zero. At any value of ω, except for certain discrete points, there is only one such solution; if L_a is this solution, it can be seen by Eqs. (12) and (14) that the other solutions L_a' and L_a'' become infinite as $\beta_{ab}\rightarrow 0$. When $\omega/\omega_{ab}=1, \frac{1}{3}, \frac{1}{5}, \cdots$ there are two solutions which remain finite. At these points we will choose the one which is used at slightly larger values of ω. The darkened curves in Fig. 1 are the values of L_a which will be used.

Since $\lambda_a+\omega_a=\beta_{ab}L_a$, λ_a approaches $-\omega_a$ for very small field strength. Equation (10) shows that all components except A_0 and B_0 then become zero, so that Eq. (17) reduces to the unperturbed solution

$$\psi=A_0e^{-i\omega_a t}+B_0e^{-i\omega_b t}.$$

Our choice of L_a thus insures that for weak enough fields A_0 will be the dominant U_a component, except near the special points $\omega/\omega_{ab}=1, \frac{1}{3}, \frac{1}{5}, \cdots$ where another component may be greater.

Up to now, we have concentrated upon obtaining a general solution of the basic differential equations which requires evaluating λ and the A's and B's in Eq. (6). In the next section, we will show how these quantities may be used directly to calculate the effects of the rf field on an observed microwave absorption line.

In molecular beam experiments the values of interest are the probabilities of finding the molecule in either state at any given time. These are equal to $|T_a|^2$ and $|T_b|^2$ in Eq. (1). From (17)

$$\begin{aligned}|T_a|^2=&|A_0|^2\sum_{k=-\infty}^{+\infty}\left(\frac{A_k}{A_0}\right)^2+|B_0|^2\sum_{l=-\infty}^{+\infty}\left(\frac{B_{-l}}{A_0}\right)^2\\&+2\sum_{\substack{k'=-\infty\\ \text{even}}}^{+\infty}\left[|A_0|^2\sum_{k=-\infty}^{+\infty}\left(\frac{A_k}{A_0}\right)\left(\frac{A_{k-k'}}{A_0}\right)\right.\\&\left.+|B_0|^2\sum_{l=-\infty}^{+\infty}\left(\frac{B_{-l}}{A_0}\right)\left(\frac{B_{-l-k'}}{A_0}\right)\right]\cos k'\omega t\\&-2|A_0||B_0|\sum_{k=-\infty}^{+\infty}\sum_{l=-\infty}^{+\infty}\frac{A_k}{A_0}\frac{B_{-k-l}}{A_0}\\&\times\cos[(\omega_a+\omega_b+2\lambda_a+l\omega)t+\theta],\end{aligned}\tag{18}$$

$$\begin{aligned}|T_b|^2=&|A_0|^2\sum_{l=-\infty}^{+\infty}\left(\frac{B_l}{A_0}\right)^2+|B_0|^2\sum\left(\frac{A_{-k}}{A_0}\right)^2\\&\times\sum_{k'=-\infty}^{+\infty}\left\{|A_0|^2\sum_{l=-\infty}^{+\infty}\frac{B_l}{A_0}\frac{B_{l-k'}}{A_0}\right.\\&\left.+|B_0|^2\sum_{k=-\infty}^{+\infty}\frac{A_{+k}}{A_0}\frac{A_{k-k'}}{A_0}\right\}\cos k'\omega t\\&+2|A_0||B_0|\sum_{l=-\infty}^{+\infty}\sum_{k=-\infty}^{+\infty}\frac{A_{-k}}{A_0}\frac{B_{k-l}}{A_0}\\&\times\cos[(\omega_a+\omega_b+2\lambda_a+l\omega)t+\theta].\end{aligned}\tag{19}$$

In Sec. 3.3 approximations are given to Eqs. (18) and (19) in which only a few terms are kept.

3.2 Discussion of General Formulas

Before discussing approximations to the somewhat cumbersome expressions given above, let us consider the physical implications of these expressions.

In the absence of the external rf field, our system consists of two energy levels having orthogonal wave functions U_a and U_b multiplied respectively by the exponential time-functions $e^{-i\omega_a t}$ and $e^{-i\omega_b t}$. When the field is turned on, the functions multiplying U_a and U_b are no longer simply exponentials, but are in general complicated periodic functions of the time which may be analyzed into a sum of exponential terms multiplied by coefficients, as in Eq. (17)

These terms will be referred to as making up a "spectrum," but not in the usual quantum-mechanical sense of a series of stationary energy states or of transitions between these states. In fact, since the interaction of the molecule with the varying external field introduces a term into the Hamiltonian which explicitly involves the time, there is really no such thing as a stationary state. Rather, there is a mixed (a,b) state whose exact form is a function of the time.

In the following sense, however, it is useful to speak of the spectrum which exists in the presence of the rf field: Assume that a second field of higher frequency is simultaneously applied to the molecule, and that this field is so weak that its effect on the states a and b is negligible compared to that of the rf field. Now assume that a third state, c, exists in the molecule, with the wave function U_c. When the frequency of the second field is resonant with the interval between c and one of the components of the mixed (a,b) state, an occasional transition will be induced which may be observed as the absorption of a photon from the second field. For example, looking at Eq. (16), absorption will occur when its frequency equals $\omega_c+\lambda_a, \omega_c+\lambda_a-2\omega, \cdots\omega_c+\lambda_a-k\omega$. The intensities of these absorptions will be proportional to $|A_0|^2, |A_2|^2\cdots, |A_k|^2$, respectively. It is assumed that the matrix element of the electric dipole

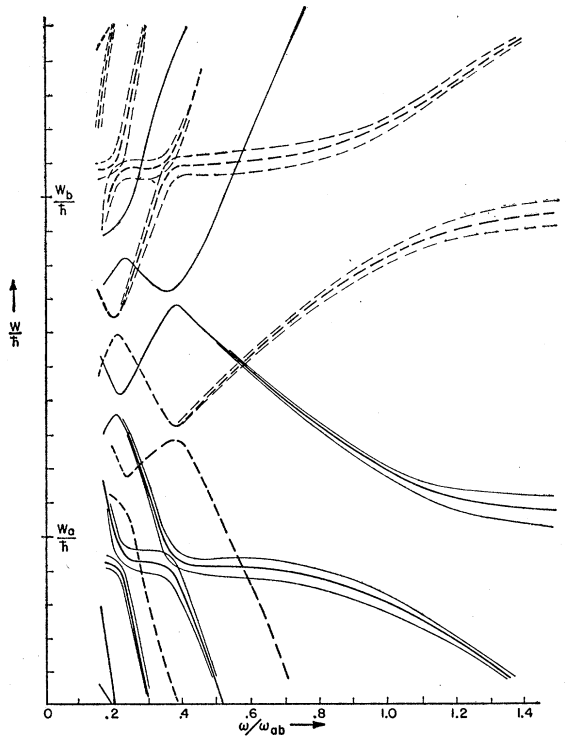

FIG. 2. The frequency spectrum of the components as a function of the applied field frequency, ω, with a field strength such that $\omega_{ab}/\beta_{ab}=5$. The frequency of a component is given by its vertical position while its intensity is roughly represented by the width assigned to it. Very weak components are represented by single lines. Components having wave function U_a are shown by solid lines and components with wave function U_b by dashed lines.

moment between U_a and U_c is not zero. If these absorption lines are observed in a spectrometer, it acts as a "spectrum analyzer" in the usual sense, i.e., an instrument to analyze the frequencies and amplitudes of the Fourier components of a time-varying quantity. This is essentially what was done in the experiment to be described in this paper; the amplitudes of the stronger components being examined critically in the frequency range near resonance.

Figure 2 shows what might be regarded as a typical spectrum. With the field intensity held constant at a moderate value ($\omega_{ab}/\beta_{ab}=5$), the positions of the various components are plotted as functions of ω/ω_{ab}. A rough indication of the relative intensity of a component is given by the thickness of the curve representing it. The solid lines represent a-type components which have the same wave function, U_a, as the unperturbed state "a". The dashed lines represent b-type components. At any particular frequency, pairs of a-type and b-type components alternate. Successive pairs are separated by twice the frequency of the applied field. At certain frequencies the separation between the two components of a pair is a minimum, and somewhere near this frequency the components have equal intensities. However, if the rf field is not too strong one component of each type is usually more intense than all the others and the position of this component changes slowly as the frequency is varied. One may roughly think of this dominant component as being the unperturbed state displaced by an average Stark effect; the other, weaker components being some sort of modulation side bands.

As discussed in the previous section, we have selected the solution of L_a which insures that A_0 will be the largest component as the field strength approaches zero, so the dominant term in the spectrum is $U_aA_0e^{i\lambda_a t}$. If the rf field is turned off, this becomes $U_aA_0e^{-i\omega_a t}$. Thus the A_0 component undergoes a Stark shift equal to $\lambda_a+\omega_a$ or $\beta_{ab}L_a$. In the presence of an actual field, however, A_0 is not dominant within small frequency ranges near $\omega/\omega_{ab}=1, \frac{1}{3}, \frac{1}{5}\cdots$. For example, if $\omega_{ab}/\beta_{ab}=5$, and $\omega/\omega_{ab}=\frac{1}{3}$, $A_{-3}/A_0=11.05$, and A_{-3} remains greater than A_0 over the range $\frac{1}{3}\leqslant\omega<0.38$. For weaker fields the frequency at which A_{-3} and A_0 are equal approaches $\omega_{ab}/3$. Similarly, A_{-5} is greater than A_0 for a range of frequencies above $\omega/\omega_{ab}=\frac{1}{5}$. At still lower frequencies several components may be greater than A_0 and the picture mentioned above breaks down altogether as the rf field becomes stronger and its frequency lower.

Our method of choosing L_a at different frequencies does not succeed in making the situation look particularly simple except for very weak fields. However, it is no more complicated than any other method which suggests itself, and it at least avoids some of the ambiguity which would arise from other choices. In Sec. 3.3, we shall obtain approximate solutions by assuming that higher components are negligible. In these solutions L_a is not many-valued and the situation is much simpler. However, for strong rf fields these complications cannot be ignored if accuracy is desired.

Figure 2 is incomplete at the low-frequency end because in this region the continued fractions converge slowly and calculations are very time-consuming. The general behavior in this range is apparent however. As ω decreases, more and more components crowd into a given frequency range on the vertical scale, and the intensity is distributed more uniformly among these components. Although there are more components having appreciable intensity, these components are still restricted to a band of width approximately $2\beta_{ab}$ about the unperturbed frequency of the levels. For several special cases at very low frequencies, it is possible to obtain simple expressions as in Sec. 3.5.

In the resonant region near $\omega/\omega_{ab}=1$, A_0 and A_{-1} are approximately equal and all other components are much smaller. An absorption line involving state "a" therefore appears to split into two nearly intense lines when the resonant rf field is turned on. This is the basis of the "resonant modulation" experiments which are fully discussed in Sec. 4.1.

The appearance of the spectrum in the high-frequency range is quite anomalous. At all the lower frequencies including dc, the most intense a-type and b-type com-

ponents lie farther apart than the unperturbed levels. But Fig. 2 shows that for $\omega \gg \omega_{ab}$ the most intense components are closer together than the unperturbed levels. Thus, the familiar "repulsion of states" which occurs in dc Stark effect becomes an "attraction of states" if a high-frequency field is used. As ω is further increased, the states return to their unperturbed positions and all effects of the field become negligible.

3.3 Approximate Solutions

If the strength of the applied field is not too great, nor its frequency too small, one can obtain useful approximate solutions which are simple functions of the physical parameters by applying Eqs. (10) and (11) and retaining only a small number of quotients in the continued fractions.

First Approximation

The simplest assumption is to approximate Eq. (11) by

$$L_a = \frac{1}{L_a + \dfrac{\omega_{ab}-\omega}{\beta_{ab}}}. \tag{20}$$

This should give a solution which is nearly correct when $\omega \approx \omega_{ab}$, for the first quotient of the first term of Eq. (11) then dominates all of the others. As can be seen in Eq. (10), this amounts to assuming that all the amplitude coefficients except A_0, B_0, A_{-1}, B_1 are negligible.

Equation (20) is quadratic in L_a and its solution is

$$L_a = -\frac{\omega_{ab}-\omega}{2\beta_{ab}} \pm \tfrac{1}{2}\left[\frac{(\psi_{ab}-\omega)^2}{\beta_{ab}{}^2}+4\right]^{\frac{1}{2}} \tag{21}$$

$$+\text{for } \omega < \omega_{ab}, \quad -\text{for } \omega \gtrless \omega_{ab}.$$

In accordance with the discussion in Sec. 3.1, the sign is chosen so that L_a remains finite as $\beta_{ab} \to 0$. It follows from (21) that:

$$\lambda_a = -\tfrac{1}{2}(\omega_a+\omega_b)+\tfrac{1}{2}\omega \pm \tfrac{1}{2}[(\omega_{ab}-\omega)^2+4\beta_{ab}{}^2]^{\frac{1}{2}}. \tag{22}$$

The relative intensities of the components may be obtained from Eqs. (10) and (21).

$$B_{+1}/A_0 = -\beta_{ab}/K_{ab}, \tag{23}$$

where

$$K_{ab} = \tfrac{1}{2}\{(\omega_{ab}-\omega) \pm [(\omega_{ab}-\omega)^2+4\beta_{ab}{}^2]^{\frac{1}{2}}\}.$$

The sign is chosen according to the same convention as for Eq. (21).

It can be seen from Eqs. (23) and (14) that in this approximation

$$\left|\frac{B_{+1}}{A_0}\right| = \left|\frac{A_{-1}}{B_0}\right| = 1$$

when $\omega = \omega_{ab}$, and this is true for all field strengths.

The expressions for $|T_a|^2$ and $|T_b|^2$ are quite simple in this approximation. Equations (18) and (19) become

$$\begin{aligned} |T_a|^2 &= |A_0|^2 + |B_0|^2(B_{+1}/A_0)^2 \\ &\quad -2|A_0||B_0|(B_{+1}/A_0) \\ &\quad \times \cos\{[(\omega_{ab}-\omega)^2+4\beta_{ab}{}^2]^{\frac{1}{2}}t+\theta\}, \\ |T_b|^2 &= |A_0|^2(B_{+1}/A_0)^2 + |B_0|^2 \\ &\quad +2|A_0||B_0|(B_{+1}/A_0) \\ &\quad \times \cos\{[(\omega_{ab}-\omega)^2+4\beta_{ab}{}^2]^{\frac{1}{2}}t+\theta\} \end{aligned} \tag{24}$$

where A_0, B_0, and θ are to be determined by the initial and normalization conditions.

Two particular sets of initial conditions are of most interest. The first is the case where a molecule was definitely known to be in a particular state, say "b," at $t=0$. If we set $|T_a|^2=0$, $|T_b|^2=1$ and $t=0$, (24) gives:

$$\theta = 0, \quad A_0 = \frac{B_{+1}/A_0}{1+(B_{+1}/A_0)^2}, \quad B_0 = \frac{1}{1+(B_{+1}/A_0)^2}. \tag{25}$$

Substituting those values into (24) and making use of (23), we get:

$$|T_a|^2 = \frac{4\beta_{ab}{}^2}{\gamma^2}\sin^2\frac{\gamma}{2}t, \quad |T_b|^2 = 1-\frac{4\beta_{ab}{}^2}{\gamma^2}\sin^2\frac{\gamma}{2}t, \tag{26}$$

where

$$\gamma = [(\omega_{ab}-\omega)^2+4\beta_{ab}{}^2]^{\frac{1}{2}}.$$

Comparison of (26) with (5) shows that they are identical when $g\mu_0 H_\perp = 2\beta_{ab}\hbar$, showing that this approximation is equivalent to assuming a rotating field as Rabi[3] did. This solution is also equal to that of Torrey.[4]

It can be seen from (26) that the molecule oscillates $\gamma/2\pi$ times each second between the two states. When $\omega=\omega_{ab}$ this oscillation frequency is $\beta_{ab}/2\pi$ which is directly proportional to the strength of the applied field. If $\omega \neq \omega_{ab}$ the oscillation frequency is greater, but the probability of finding the system in state "a" never reaches one before it starts to decrease again.

Equation (17) can now be written

$$\begin{aligned} \psi = &\frac{\beta_{ab}}{\gamma} U_a e^{-\frac{1}{2}i(\omega_a+\omega_b)t}\{e^{\frac{1}{2}i(\omega+\gamma)t} - e^{\frac{1}{2}i(\omega-\gamma)t}\} \\ &-\frac{\beta_{ab}}{\gamma} U_b e^{-\frac{1}{2}i(\omega_a+\omega_b)t}\left\{\frac{\beta_{ab}}{K_{ab}}e^{\frac{1}{2}i(-\omega+\gamma)t} + \frac{K_{ab}}{\beta_{ab}}e^{-\frac{1}{2}i(\omega+\gamma)t}\right\}. \end{aligned} \tag{27}$$

Equations (26) and (27) have been derived by assuming a system of molecules known to be in state "b" at $t=0$, a situation which might occur in the case of a molecular beam which has been prepared so that this initial condition holds for all the molecules in the beam.

However, the conditions which must be applied in the "resonant modulation" experiment are somewhat different. Here we have a gas in a wave guide; the

molecules of the gas are colliding with each other and the walls of the wave guide at random and have different histories although they are all influenced by the same rf field. All that we can say about a particular molecule is that at a given time it is equally likely to be either of the two independent states possible in the presence of the rf field. Thus, $|A_0|=|B_0|$ while the phase angle θ is undetermined. If this condition is applied and (24) normalized,

$$|T_a|^2+|T_b|^2=1=2|A_0|^2[1+(B_{+1}/A_0)^2]$$

giving

$$|A_0|=\frac{1}{\sqrt{2}}\frac{1}{[1+(B_{+1}/A_0)^2]^{\frac{1}{2}}}=|B_0|. \tag{28}$$

This, together with (23) gives

$$\begin{aligned}|T_a|^2&=\tfrac{1}{2}\{1-(2\beta_{ab}/\gamma)\cos(\gamma t+\theta)\},\\ |T_b|^2&=\tfrac{1}{2}\{1+(2\beta_{ab}/\gamma)\cos(\gamma t+\theta)\},\end{aligned} \tag{29}$$

where θ is indeterminate for any particular molecule. In considering the entire ensemble of molecules an average must be taken over all values of θ. Equation (29) then shows that at any time there are equal numbers of molecules in the two states.

Equation (17) now becomes

$$\psi=U_a\frac{e^{-\frac{1}{2}i(\omega_a+\omega_b)t}}{\sqrt{2}\gamma K_{ab}}\{K_{ab}e^{\frac{1}{2}i(\omega+\gamma)t}-e^{-i\theta}\beta_{ab}e^{\frac{1}{2}i(\omega-\gamma)t}\}$$

$$-\frac{U_be^{-\frac{1}{2}i(\omega_a+\omega_b)t}}{\sqrt{2}\gamma K_{ab}}\{\beta_{ab}e^{\frac{1}{2}i(-\omega+\gamma)t}+e^{-i\theta}K_{ab}e^{-\frac{1}{2}i(+\omega+\gamma)t}\}. \tag{30}$$

In this form it is easy to determine the spectrum as discussed in Sec. 3.2. If there is a third stationary state of the unperturbed system, having the wave function U_c and for which $|\langle a|\mathfrak{y}\cdot\mathbf{E}|c\rangle|^2$ does not vanish, transitions to this state may be induced by a weak oscillating field of the right frequency. Equation (30) shows that this will occur at two frequencies separated by $\gamma/2\pi$ sec^{-1} and with relative probabilities $|K_{ab}/\beta_{ab}|^2$. Thus, the $a\rightarrow c$ spectrum which is a single line in the unperturbed system splits into two components in this approximation. Absorption lines involving state b will be similarly split. When $\omega=\omega_{ab}$, $K_{ab}=\beta_{ab}=\gamma/2$ so the spectrum of a-type states consists of two equally intense components which are separated in angular frequency by $2\beta_{ab}$ sec^{-1}. The separation of the two components is thus proportional to the intensity of the perturbing field, but their relative amplitudes is independent of it.

When $\omega<\omega_{ab}$, $K_{ab}>\beta_{ab}$ and one component is more intense; however, when $\omega>\omega_{ab}$, $K_{ab}<\beta_{ab}$ and the intensities are interchanged. Thus it appears that ω_{ab} may be determined by varying the frequency of the rf field and observing when the two components are equally intense. In higher approximations this relationship does not hold exactly; the extent of deviation from it depends upon the intensity of the applied field as discussed below.

Second Approximations

The preceding solution is valid only for relatively weak fields with the frequency near resonance. It is simple to find a solution which is valid over a much wider range, including intermediate and high-frequency fields, and which reduces to the previous one near resonance.

Equation (11) converges rapidly when β_{ab}/ω_{ab} and β_{ab}/ω are $\ll 1$. To the first power in these quantities it can be written:

$$L_a=\frac{1}{L_a+\dfrac{\omega_{ab}-\omega}{\beta_{ab}}+\dfrac{\beta_{ab}}{2\omega}}+\frac{\beta_{ab}}{\omega_{ab}+\omega}. \tag{31}$$

Ignoring L_a in some of the denominators is justified if we require a solution for which $L_a\ll\omega/\beta_{ab}$. Equation (31) may be further simplified to

$$L_a^2+L_a\frac{\omega_{ab}-\omega}{\beta_{ab}}-\frac{2\omega_{ab}}{\omega_{ab}-\omega}=0, \tag{32}$$

which has the solutions

$$L_a=-\frac{\omega_{ab}-\omega}{2\beta_{ab}}\pm\frac{1}{2}\left[\frac{(\omega_{ab}-\omega)^2}{\beta_{ab}^2}+4+4\frac{\omega_{ab}-\omega}{\omega_{ab}+\omega}\right]^{\frac{1}{2}}. \tag{33}$$

This differs from Eq. (21) only in the last term inside the brackets, and the same sign conventions are used. Plots of Eq. (33) for several field strengths are given by the dotted curves in Fig. 1. It can be seen that Eq. (33) is a better approximation at the weaker field, but does not show up the multiplicity of solutions or their rapid variations in certain regions.

The amplitude coefficients are:

$$\begin{aligned}\frac{B_{+1}}{A_0}&=-\frac{A_{-1}}{B_0}=\frac{-1}{L_a+\dfrac{\omega_{ab}-\omega}{\beta_{ab}}+\dfrac{\beta_{ab}}{2\omega}},\\ \frac{B_{-1}}{A_0}&=-\frac{A_{+1}}{B_0}=\frac{-\beta_{ab}}{\omega_{ab}+\omega},\\ \frac{A_{+2}}{A_0}&=-\frac{B_{-2}}{B_0}=\frac{\beta_{ab}}{2\omega}\frac{B_{+1}}{A_0},\end{aligned} \tag{34}$$

where L_a is given by Eq. (33).

Very close to resonance when $|\omega_{ab}-\omega|\ll\beta_{ab}$, Eq. (33) approaches (21), the rotating field solution. Even for $\omega=\omega_{ab}$, however, the counter-rotating component makes its presence felt on the amplitude coefficients. Thus, $B_{+1}/A_0\approx 1+(\beta_{ab}/2\omega)$ when $\omega=\omega_{ab}$, showing that the components A_0 and A_{-1} are not quite equal at resonance

in this approximation. Far from resonance where

$$\frac{(\omega_{ab}-\omega)^2}{\beta_{ab}^2} \gg \frac{8\omega_{ab}}{\omega_{ab}+\omega}, \tag{35}$$

Eq. (33) becomes

$$L_a \approx \frac{\beta_{ab}}{\omega_{ab}+\omega} + \frac{\beta_{ab}}{\omega_{ab}-\omega}. \tag{36}$$

The condition of Eq. (35) may be satisfied for fairly strong fields when $\omega > \omega_{ab}$ but only for much weaker fields when $\omega \ll \omega_{ab}$. In addition, the previous condition for this approximation, $\beta_{ab}/\omega \ll 1$, must still be met.

In the intermediate and low-frequency ranges, Eq. (36) or (33) gives a single-valued solution for L_a to replace the complicated one in Fig. 1. This should be adequate except when it is possible to resolve a frequency difference as small as that between A_0 and A_{-3} at their closest approach (Fig. 2).

Better Approximations

To extend the solutions to include terms of order β_{ab}^2/ω^2 and $\beta_{ab}^2/\omega_{ab}^2$ Eq. (11) is approximated by

$$L_a = \frac{1}{L_a + \dfrac{\omega_{ab}-\omega}{\beta_{ab}} - \dfrac{1}{L_a - \dfrac{2\omega}{\beta_{ab}}}} + \frac{1}{L_a + \dfrac{\omega_{ab}-\omega}{\beta_{ab}}}. \tag{37}$$

All other terms make contributions of third order or higher. It has already been shown that L_a is of zero order near resonance and first order elsewhere. It is only in the resonance region that the additional terms in Eq. (37) give rise to a correction term in the solution for L_a. This solution, obtained in the Appendix 3.3a, is

$$L_a = \rho\left[1 - \frac{\beta_{ab}^2}{4\omega_{ab}^2}\frac{2\rho^2-1}{\rho^2+1}\right], \tag{38}$$

where ρ is the solution for L_a given in Eq. (33). The factor $(2\rho^2-1)/(\rho^2+1)$ varies from $\frac{1}{2}$ to 0 as $|\rho|$ runs from one to $1/\sqrt{2}$. Equation (38) may be used in the region near resonance for which $2\rho^2-1>0$, but outside this range the correction terms is disregarded.

A more accurate solution would retain more of the fractions in Eq. (11) and include terms of higher order in β_{ab}/ω_{ab} and β_{ab}/ω. Third-order terms should show up the rapid variations seen in Fig. 1(b) near $\omega/\omega_{ab} \approx 0.40$; which are associated with the vanishing of $(\omega_{ab}-3\omega)/\beta_{ab}$ in Eq. (11). It would be necessary to retain fifth-order terms to represent in detail the behavior near $\omega/\omega_{ab} = 0.23$.

Since the amount of algebra increases very rapidly with the power of the solution, further calculations have been done numerically. Figures 1 and 2 are based on these results as are the magnitudes of L_a and the amplitude coefficients near resonance. The following procedure was used in calculating each point: A trial value of L_a was used and the two continued fractions in (11) were computed, using two or three denominators in each. If the sum of these two fractions did not give the original trial value of L_a, a new value between the two was tried. This was continued until the trial value of L_a and the computed value agreed to within one digit in the second figure after the decimal point. This procedure was then repeated using several additional denominators. When the result was unaffected by using two additional denominators, the last value calculated was considered final. The subfractions computed in this final calculation were recorded, for they represent the values of $B_{\pm1}/A_0$, $A_{\pm2}/B_{\pm1}$, etc. This can be seen by comparing Eqs. (10) and (11).

3.4a Solution Near Resonance

In this section, we will give a detailed discussion of the solution including terms of second order in β_{ab}/ω_{ab} and β_{ab}/ω. Expressions will be obtained for the relative amplitudes of the components and a condition given for equal intensity of the two main components into which a level splits near resonance.

Making use of Eqs. (10) and (38),

$$\frac{B_{+1}}{A_0} = \frac{-\beta_{ab}}{\rho + \dfrac{\omega_{ab}-\omega}{\beta_{ab}} - \rho\dfrac{2\rho^2-1}{\rho^2+1} - \dfrac{1}{\rho - \dfrac{2\omega}{\beta_{ab}}}}, \tag{39}$$

which can be rewritten,

$$\frac{B_{+1}}{A_0} = \frac{-\beta_{ab}}{K_{ab} + \dfrac{\beta_{ab}^2}{2\omega} + \dfrac{\beta_{ab}^2}{4\omega_{ab}^2}\dfrac{2-\rho^2}{1+\rho^2}\rho}, \tag{40}$$

where

$$K_{ab} = +(\omega_{ab}-\omega)+\beta_{ab}\rho = \frac{\omega_{ab}-\omega}{2} \pm \frac{1}{2}\left[(\omega_{ab}-\omega)^2 + \frac{8\omega_{ab}\beta_{ab}^2}{\omega_{ab}+\omega}\right]^{\frac{1}{2}}.$$

Use + if $\omega < \omega_{ab}$ and − if $\omega \geqslant \omega_{ab}$. To second order, we may now write

$$\frac{B_{+1}}{A_0} = -\frac{\beta_{ab}}{K_{ab}}\left[1 - \frac{\beta_{ab}}{2\omega}\frac{\beta_{ab}}{K_{ab}} + \frac{\beta_{ab}^2}{4\omega_{ab}^2}\left(\frac{\beta_{ab}^2}{K_{ab}^2} - \frac{2-\rho^2}{1+\rho^2}\frac{\rho}{K_{ab}}\beta_{ab}\right)\right], \tag{41}$$

and

$$\left(\frac{B_{+1}}{A_0}\right)^2 = \frac{\beta_{ab}^2}{K_{ab}^2}\left[1 - \frac{\beta_{ab}}{\omega}\frac{\beta_{ab}}{K_{ab}} + \frac{\beta_{ab}^2}{4\omega_{ab}^2} \times \left(\frac{3\beta_{ab}^2}{K_{ab}^2} - 2\frac{2-\rho^2}{1+\rho^2}\frac{\rho}{K_{ab}}\beta_{ab}\right)\right]. \tag{42}$$

The other components are shown in Appendix 3.4a to be

$$\begin{aligned}
&\frac{B_{-1}}{A_0}=-\frac{A_{+1}}{B_0}=-\left[\frac{\beta_{ab}}{2\omega_{ab}}+\frac{\beta_{ab}^2}{4\omega_{ab}^2}\left(\frac{\omega_{ab}-\omega}{\beta_{ab}}-\rho\right)\right],\\
&\frac{A_{+2}}{A_0}=+\frac{B_{-2}}{B_0}=\frac{B_{+1}}{A_0}\left[\frac{\beta_{ab}}{2\omega_{ab}}+\frac{\beta_{ab}}{4\omega_{ab}^2}\left(2\frac{\omega_{ab}-\omega}{\beta_{ab}}+\rho\right)\right],\\
&\frac{B_{+3}}{A_0}=-\frac{A_{-3}}{B_0}=-\frac{A_{+2}}{A_0}\frac{\beta_{ab}}{\omega_{ab}-3\omega}=\frac{B_{+1}}{A_0}\frac{\beta_{ab}^2}{4\omega_{ab}^2},\\
&\frac{A_{-2}}{A_0}=\frac{B_{+2}}{B_0}=+\frac{\beta_{cb}^2}{4\omega_{ab}^2}.
\end{aligned}\tag{43}$$

We define the "splitting," γ, as the angular frequency separating the components A_0 and A_{-1} or B_0 and B_{+1} near resonance when they have approximately equal intensities. Equation (17) shows that A_0 and A_{-1}, the two predominant a-type components, have relative amplitudes B_{+1}/A_0 and are separated by

$$\gamma=2\beta_{ab}L_a+\omega_{ab}-\omega.\tag{44}$$

Now make use of Eqs. (38) and (33)

$$\begin{aligned}
&\gamma=2\beta_{ab}\rho\left[1-\frac{\beta_{ab}^2}{4\omega_{ab}^2}\frac{2\rho^2-1}{\rho^2+1}\right]+\omega_{ab}-\omega,\\
&|\gamma|=\beta_{ab}\left\{\left[\frac{(\omega_{ab}-\omega)^2}{\beta_{ab}^2}+\frac{8\omega_{ab}}{\omega_{ab}+\omega}\right]^{\frac{1}{2}}-\frac{\beta_{ab}^2}{2\omega_{ab}^2}\frac{2\rho^2-1}{\rho^2+1}\right\}.
\end{aligned}\tag{45}$$

At $\omega=\omega_{ab}$

$$|\gamma|=2|\beta_{ab}|\left[1-\frac{\beta_{ab}^2}{8\omega_{ab}^2}\right].$$

Equation (24) shows that the amplitude with which the molecule oscillates between states a and b is proportional to $A_0B_0(B_{+1}/A_0)$. In the case where a molecule is initially known to be in one of the states this amplitude is, from Eq. (25), $(B_{+1}/A_0)^2[1+(B_{+1}/A_0)^2]^{-1}$ which has a maximum when $B_{+1}/A_0=1$. The frequency at which this occurs may be obtained by setting $B_{+1}/A_0=1$ in Eq. (50) of Sec. 4.2. Solving this equation gives the condition for resonance:

$$\frac{\omega}{\omega_{ab}}=1+\frac{\beta_{ab}^2}{\omega_{ab}^2},\tag{46}$$

where $\hbar\omega_{ab}$ is the energy difference between the two levels. As was pointed out in Sec. 2.4, this result has been obtained by Bloch and Siegert.[5] For stronger fields, the shift in resonance may be calculated numerically from Eqs. (10) and (11) by determining at each field strength the frequency at which B_{+1}/A_0 equals one.

3.5 Low-Frequency Perturbation

If the frequency of the rf field is low enough, the problem may be treated quasistatically as outlined in Sec. 2.6. We will first consider the part of the solution which reduces to state "a" at zero rf field intensity.

For a dc electric field, the solution is

$$\psi=N\left[U_a-\frac{4\beta_{ab}}{+(\omega_{ab}/2)+\frac{1}{2}(\omega_{ab}^2+16\beta_{ab}^2)^{\frac{1}{2}}}U_b\right]\times\exp\left\{i\left[\frac{\omega_a+\omega_b}{2}-\tfrac{1}{2}(\omega_{ab}^2+16\beta_{ab}^2)^{\frac{1}{2}}\right]t\right\},\tag{47}$$

where N is a normalization factor. If the frequency is small and $\beta_{ab}\ll\omega_{ab}$, we may replace β_{ab} by $\beta_{ab}\cos\omega t$. Then

$$\begin{aligned}
&U_a\sum A_k e^{i(\lambda_a-k\omega)t}\\
&\approx NU_a e^{i\omega_a t}\exp\left(-i\int_0^t\frac{4\beta_{ab}^2\cos^2\omega t}{\omega_{ab}}dt\right)\\
&\approx NU_a\exp\left[i\left(\omega_a-\frac{2\beta_{ab}^2}{\omega_{ab}}\right)t\right]\exp\left[-i\frac{\beta_{ab}^2}{\omega_{ab}}\frac{\sin2\omega t}{\omega}\right].
\end{aligned}$$

Clearly $\lambda_a=\omega_a-(2\beta_{ab}^2/\omega_{ab})$, and

$$A_n=\frac{1}{2\pi}N\int_{-\pi}^{\pi}\exp\left[i\left(2n\omega t-\frac{\beta_{ab}^2}{\omega_{ab}}\frac{\sin2\omega t}{\omega}\right)\right]d(2\omega t),$$

where k is any even integer and n any integer. The integral is familiar, and A_n may be written

$$A_n=NJ_n\left(\frac{\beta_{ab}^2}{\omega_{ab}\omega}\right).$$

Thus the U_a wave function has a spectrum given by

$$\sum_{n=-\infty}^{+\infty}J_n\left(\frac{\beta_{ab}^2}{\omega_{ab}\omega}\right)e^{-2in\omega t}\exp\left[i\left(\omega_a-\frac{2\beta_{ab}^2}{\omega_{ab}}\right)t\right]$$

showing the frequency-shift of the main component and the side bands, whose intensities fall off as

$$|J_n(\beta_{ab}^2/\omega\omega_{ab})|^2.$$

This is the solution for second-order Stark effect described and observed by Townes and Merritt.[8]

For first-order Stark effect, by setting $\omega_{ab}=0$ in Eq. (47) and proceeding as before one can show that the main component is unshifted while the side bands are separated by the ω instead of 2ω and fall off as $|J_n(2\beta_{ab}/\omega)|^2$. When ω_{ab} and β_{ab} are of comparable magnitude, there are no such simple expressions for the positions and intensities of the components.

IV. RESONANT MODULATION

4.1 Discussion of Resonant Modulation Experiment in OCS

Measurements were carried out near resonance to check the theory and also to determine the practicality of using resonant modulation as a precision method of determining the energy difference between certain molecular levels. For instance, one might wish to determine the interval between two hyperfine levels corresponding to the same rotational angular momentum by observing a microwave transition to another rotational state while inducing transitions between the hyperfine levels by an rf field.

As a first test, however, it was decided to use the *l*-type doublets of the linear molecule OCS (carbonyl sulfide). These levels satisfy our assumption of isolated pairs of states and also provide fairly strong microwave absorption lines to observe. They are also uncomplicated by nuclear interactions.

Figure 3(a) shows the levels of the OCS molecule which are of interest. The measured microwave frequencies of the two allowed transitions $a \rightarrow c$ and $b \rightarrow d$ are indicated on the diagram. The energy intervals (a, b) and (c, d) are much smaller; they arise from the vibration-rotation interaction in which coriolis forces remove the degeneracy between the two orthogonal bending vibrations of the linear OCS molecule.[11] These interactions increase with rotational angular momentum, J, as $J(J+1)$ so the (c, d) separation should be three times as great as for (a, b). On the basis of this assumption, and previous measurements[12] of the frequencies $a \rightarrow c$ and $b \rightarrow d$, the (a,b) and (c,d) separations are determined to be 12.76 Mcps and 38.28 Mcps respectively.

The resonant modulation experiment is carried out by observing the two absorption lines $a \rightarrow c$ and $b \rightarrow d$ in a conventional Stark-type[13] microwave spectroscope while the rf field is applied to the molecules. A schematic diagram of the apparatus is shown in Fig. 5. With the OCS gas at a pressure of about 10^{-2} mm in the wave guide of the spectroscope, an rf field with an amplitude of several volts is applied to the same septum as the 100 kc square-wave voltage used in spectrometers of this type. This subjects the gas to a fairly uniform rf field of the order of 10 volts-cm intensity. The 100 kc square-wave Stark voltage simultaneously applied to the septum plays no part in the resonant modulation process, but is merely part of the microwave detection system.

When the frequency, ν, of the rf voltage is near either ν_{ab} or ν_{cd}, each absorption line appears to split into two components. The relative intensity of these components is sensitive to the frequency of the rf field, and

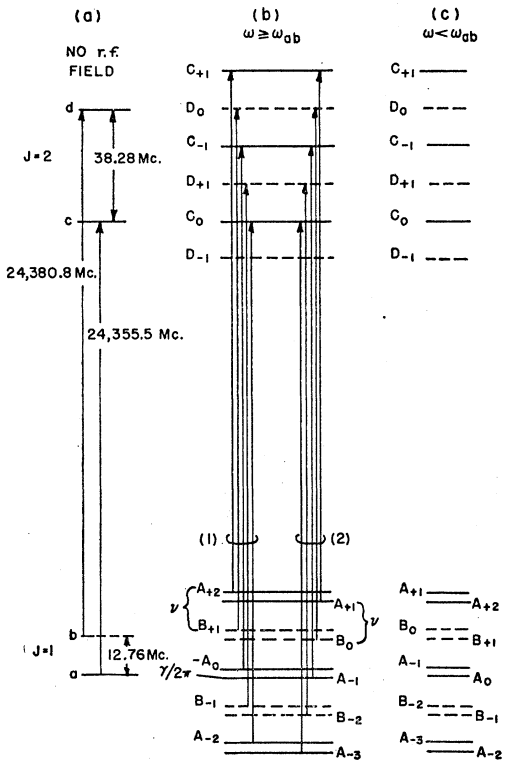

FIG. 3. (a) The unperturbed OCS energy levels of interest in the resonance modulation experiment. (b) The components are shown when the applied field frequency is slightly above resonance. The transition within groups (1) and (2) occur at the same microwave frequency. (c) The components are shown relabeled according to our convention when $\omega > \omega_{ab}$.

if the strength of the field is held constant while its frequency is varied through resonance, first one and then the other component becomes more intense. This is illustrated in Fig. 2.

In the first approximation, valid for weak rf fields, the relative intensity of the two components is independent of the amplitude of the field, the two components being equally intense when ν is exactly equal to ν_{ab} or ν_{cd}. This suggests that one could measure ν_{ab} directly by determining the rf frequency at which the two components are equally intense. However, the higher approximations in Sec. 3.3 predict, and experimental results confirm, that for greater rf field strength the relative intensity of the components depends upon field strength as well as frequency. One would like to use as weak a field as possible in order to minimize the dependence on field intensity and also because, as discussed in Sec. 4.3, the resonance is sharper for weak fields and one could expect to measure ν_{ab} more accurately. However, as the field strength is decreased, the separation of the components also decreases. Although it has been assumed in the theory that the lines are perfectly sharp, they, of course, actually have a finite width, in our case about $\frac{1}{2}$ megacycle, due mainly to pressure broadening. If the intensities of the components

[11] H. H. Nielsen, Revs. Modern Phys. **23**, 90 (1951).
[12] P. Kisliuk and C. H. Townes, Table of Microwave Lines, National Bureau of Standards Circular 518, 1952 (unpublished).
[13] R. H. Hughes and E. B. Wilson, Phys. Rev. **71**, 562 (1947).

are to be compared their separation must be comparable to this line width, which sets a lower limit on the rf voltage which can be employed.

A Stark-type microwave spectrometer, while sensitive, is not very well adapted to measuring intensities of absorption lines. It was therefore desirable to minimize difficulties by confining all intensity comparisons to deciding when two components were equally intense. The experimental procedure was to hold constant the intensity of the rf voltage as measured on a vacuum-tube voltmeter and then vary the oscillator frequency until the two components appeared equally intense. This frequency was recorded as ν_0, the rf voltage changed and the process repeated. In this way, a plot of ν_0 as a function of field strength was made which, when extrapolated to zero field strength, gives the actual value of ν_{ab}. This complicated procedure might be simplified if one knew the relationship between ν_0 and the field strength. It might then be possible to determine ν_{ab} with only one or two measurements. In this connection two problems need to be discussed, one theoretical and one experimental.

The first is that in our experiment, one does not observe the perturbed spectrum of a pair of levels by means of transitions to a state which is completely unaffected by the rf field. For example, when observing the $a \rightarrow c$ transition (Fig. 3) in the presence of an rf field which is resonant with ν_{ab}, the field affects states "c" and "d" as well as "a" and "b." Although the effect of the rf field on "c" will not be so great as on "a" because ν is not resonant with ν_{cd}, it may still be great enough to change the results and must be calculated. This is done in the next section.

The experimental difficulty arose from the fact that we were unable to make a reliable measurement of the amplitude of the rf voltage. Equation (45) relates the separation of the two components, or "splitting" to the amplitude of the applied voltage, assuming that one knows the matrix element between states a and b. The matrix elements in this case can be calculated[11] and an experimental check of the above relation gave a discrepancy of the order of 30%. It was assumed that this discrepancy was due to the vacuum-tube voltmeter giving an incorrect reading of the actual effective voltage across the wave guide. Smaller inconsistencies between separate measurements of the voltage also indicated that they were unreliable. As the basic purpose of this experiment was to study the behavior of "resonant modulation," rather than to measure frequency intervals, it was decided that the "splitting" itself would be used as means of determining the voltage. This "splitting" then was directly measured by using a microwave frequency standard. This is a rather inconvenient procedure which in effect nullifies one of the advantages of using resonant modulation; namely, the ability to make frequency measurements in the rf rather than the microwave range. It seems likely that a way to make reliable voltage measurements could be found and the need for a microwave frequency standard eliminated.

4.2 Theory of Resonant Modulation in OCS

Figure 3(b) shows the spectrum of the l-type doublets of OCS when subjected to an rf field resonant with ν_{ab}. The spectrum of the (a, b) state is characteristic of the resonant condition. The (c, d) spectrum is nonresonant since $\nu \approx \nu_{cd}/3$. All the A components have the same wave function, $U_a(x,y,z)$, as the unperturbed "a" state. Similarly, the B, C, and D components have the wave functions of the other unperturbed states.

The components A_0 and A_{-1}, B_0, and B_{+1} are about equally intense and occur in pairs which are "split" by a frequency difference which is very nearly proportional to the rf field intensity. The magnitude of this "splitting" is given in Eq. (45). The weaker components such as A_{+2} and A_{+1}, B_{-2}, and B_{-1} also occur in pairs of approximately equal intensity. In the upper state the intense C_0 and D_0 components are shifted relatively little from their unperturbed positions, while the other components are weaker by a factor of the order β_{cd}/ω_{cd}.

For the l-type doublets, the matrix elements of the dipole moment vanish, except between the states a and c or b and d. Therefore, as shown in Fig. 3(a), only two microwave absorption lines are observed when there is no rf field. In the presence of the field, corresponding to each of these lines, absorption occurs at two different microwave frequencies which are separated by the "splitting" frequency, $\gamma/2\pi$. There are many pairs of components separated by each of these frequencies, but we will consider only the five pairs for which the microwave absorption varies as the second power or lower of the rf field. The problem is to calculate the precise frequency, ν_0 at which transitions (1) and (2) are equally intense.

In absorption spectroscopy, the radiation used is usually so weak that it induces transitions in the absorbing atoms or molecules of a gas at a much lower rate than collisions occur between the molecules. As discussed in Sec. 2.2, the radiation then produces very little change in the relative populations of the molecular states. Under these conditions the fraction of the radiation absorbed at the peak of an absorption line is independent of the intensity of the radiation and is proportional to $|\langle\psi_a|\mu|\psi_c\rangle|^2$ where $\langle\psi_a|\mu|\psi_c\rangle$ is the matrix element of the electric or magnetic dipole moment between the initial and final states. For example, in Fig. 3(a) microwave absorption lines are shown for the transitions from state a to c and from b to d, when there is no rf field. The electric dipole matrix elements and hence intensities of these lines are equal.

In the presence of the rf field, the $J=1$ state has the wave function

$$\Psi_{ab} = U_a T_a(t) + U_b T_b(t),$$

where $T_a(t)$ and $T_b(t)$ may be analyzed into Fourier components as in Eq. (16). Similarly the $J=2$ state

has the wave function

$$\Psi_{cd}=U_cT_c(t)+U_dT_d(t).$$

Figure 3(b) shows the "spectrum" corresponding to those two complex states when ω is slightly greater than ω_{ab}. Each horizontal line represents a Fourier component of T_a, T_b, T_c, or T_d; its frequency is indicated by the vertical position of the line.

When the rf field is on, the probability of a $J=1\rightarrow 2$ transition is still proportional to the square of the dipole matrix element between the initial and final states, although these are no longer stationary states. Thus the absorption is proportional to

$$|\langle\Psi_{ab}|\,\mathfrak{y}\cdot\mathbf{E}_me^{i\omega mt}|\,\Psi_{cd}\rangle|^2,$$

where $\mathbf{E}_me^{i\omega mt}$ is the microwave field. In Fig. 3(b), we see that components B_{+1} and D_0 are separated by the same frequency as A_0 and C_{-1}, B_{-1} and D_{+1}, etc. If the microwave frequency is adjusted to resonate with this frequency, absorption occurs which is proportional to

$$|(B_{+1}D_0+B_{-1}D_{+1})\beta_{bd}+[A_0C_{-1}+B_{-1}D_{+1}+A_{-2}C_0)\beta_{ac}|^2,$$

Other pairs of components which are separated by the same frequency are disregarded here because their contribution is small. The intensity of transition (2), which occurs at a frequency $\gamma/2\pi$ greater, is given by a similar expression. For this set of levels $\beta_{bd}=\beta_{ac}$, which may be derived from the theory of the l-type doublets but is also demonstrated by the fact that the two microwave lines are observed to be equally intense when there is no rf field.

The condition that the two absorption lines (1) and (2) be equally intense may be written

$$\begin{aligned}&A_{+2}C_{+1}+B_{+1}D_0+A_0C_{-1}+B_{-1}D_{+1}+A_{-2}C_0\\&\quad=A_{+1}C_{+1}+B_0D_0+A_{-1}C_{-1}+B_{-2}D_{+1}+A_{-3}C_0.\end{aligned}\tag{48}$$

Divide Eq. (46) by D_0 and make use of the relations between coefficients in Eq. (15). Also set $A_0=B_0$ and $C_0=D_0$. Then

$$\begin{aligned}&\frac{B_{+1}}{A_0}-\frac{D_{+1}}{C_0}+\frac{B_{-1}}{A_0}\frac{D_{+1}}{C_0}+\frac{A_{-2}}{A_0}-\frac{A_{+2}}{A_0}\frac{D_{-1}}{C_0}\\&\quad=1-\frac{B_{+1}}{A_0}\frac{D_{+1}}{C_0}\frac{A_{+2}}{A_0}\frac{D_{+1}}{C_0}-\frac{B_{+3}}{A_0}\frac{B_{-1}}{A_0}\frac{D_{-1}}{C_0}.\end{aligned}\tag{49}$$

Now, making use of such identities as

$$B_{+3}/A_0=(B_{+3}/A_{+2})(A_{+2}/B_{+1})(B_{+1}/A_0),$$

we obtain

$$\begin{aligned}&\frac{B_{+1}}{A_0}\left[1-\frac{D_{+1}}{C_0}+\frac{B_{+3}}{A_{+2}}\frac{A_{+2}}{B_{+1}}-\frac{A_{+2}}{B_{+1}}\frac{D_{+1}}{C_0}-\frac{A_{+2}}{B_{+1}}\frac{D_{-1}}{C_0}\right]\\&\quad=1-\frac{D_{+1}}{C_0}-\frac{A_{-2}}{B_{-1}}\frac{B_{-1}}{A_0}-\frac{B_{-1}}{A_0}\frac{D_{+1}}{C_0}+\frac{B_{-1}}{A_0}\frac{D_{-1}}{C_0}.\end{aligned}\tag{50}$$

The formulas for the A and B coefficients, which apply in the resonance region, are given in Eqs. (41)–(44). The C and D coefficients may be obtained from Eqs. (34) by replacing a by c and A by C; also b by d and B by D. For example, corresponding to $B_{-1}/A_0=-\beta_{ab}/\omega_{ab}+\omega$ one obtains $D_{-1}/C_0=-\beta_{cd}/\omega_{cd}+\omega$.

We will substitute the appropriate expressions for the coefficients into (49) and solve for the frequency, ω_0, at which transitions (1) and (2) are equally intense. In Eq. (50), B_{+1}/A_0 is approximately equal to one; but the other coefficients are smaller, being of the order β_{ab}/ω_{ab} or β_{cd}/ω_{cd}.

In Appendix 4.2a, it is shown that near resonance Eq. (41) can be simplified to

$$\frac{B_{+1}}{A_0}=1+\frac{\beta_{ab}}{2\omega_{ab}}+\frac{\beta_{ab}^2}{8\omega_{ab}^2}+\frac{\omega_{ab}-\omega}{\beta_{ab}}\left(\frac{1}{2}+\frac{\beta_{ab}}{4\omega_{ab}}\right)+\frac{1}{8}\frac{(\omega_{ab}-\omega)^2}{\beta_{ab}^2},\tag{51}$$

where terms up to the second power of the field strength have been kept. Equation (50) is then solved, giving

$$\omega_0=\omega_{ab}+\frac{5}{3}\frac{\beta_{ab}^2}{\omega_{ab}}+\frac{4\beta_{ab}\beta_{cd}}{\omega_{cd}-\omega_{ab}}+\frac{\beta_{ab}^3}{\omega_{ab}^2}+\frac{2\beta_{ab}^2\beta_{cd}}{\omega_{ab}(\omega_{cd}-\omega_{ab})}.\tag{52}$$

For the l-type doublets[11] in OCS, $\beta_{cd}=\beta_{ab}/3$ and $\omega_{cd}=3\omega_{ab}$. Equation (52) can then be written

$$\nu_0=\nu_{ab}+\frac{5}{3\nu_{ab}}\left(\frac{\beta_{ab}}{2\pi}\right)^2+\frac{4}{3\nu_{ab}^2}\left(\frac{\beta_{ab}}{2\pi}\right)^3.\tag{53}$$

The measured quantities in our experiment were ν_0 and the "splitting," γ. By solving Eq. (45) for β_{ab} as an explicit function of γ, one obtains

$$\frac{\beta_{ab}}{2\pi}=\frac{\gamma/2\pi}{2\left[1+\dfrac{(2\pi)^2(\nu_{ab}-\nu)^2}{\gamma^2}+\dfrac{\nu_{ab}-\nu}{2\nu_{ab}}-\dfrac{\gamma^2}{64\pi^2\nu_{ab}^2}\right]^{\frac{1}{2}}}.\tag{54}$$

Figure 4 is a plot of the measured values of ν_0 against $\beta_{ab}/2\pi$. The values of β_{ab} were obtained by measuring the "splitting" with the aid of a microwave frequency standard and then using Eq. (54). The theoretically predicted curve for ν_0 as a function of β_{ab} is also shown in Fig. 4.

If ν_{ab} is set equal to 12.78 Mc, Eq. (53) becomes

$$\nu_0=12.78+0.131\left(\frac{\beta_{ab}}{2\pi}\right)^2+0.0082\left(\frac{\beta_{ab}}{2\pi}\right)^3.\tag{55}$$

4.3 Stark Effect Above Resonance

In Sec. 3.2, it was mentioned that when $\omega>\omega_{ab}$ the separation of the states appears to be less than in the absence of the field; this can now be proved. Equation (36) shows that L_a is negative above resonance and it follows from the definition of L_a that the A_0 and B_0 components are separated by less than ω_{ab}. In addition,

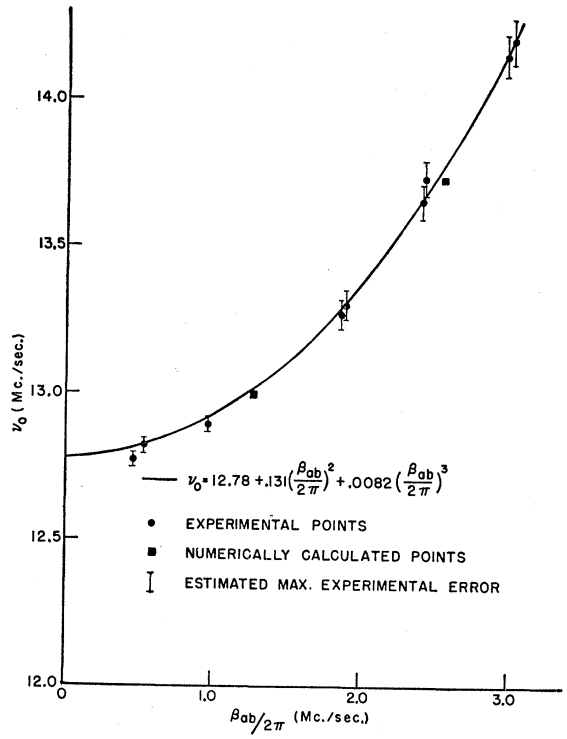

FIG. 4. Measured and calculated values of ν_0 as a function of the field intensity.

by Eq. (34), A_{-1} and B_{+1} are seen to become small when $\omega \gg \omega_{ab}$, showing that A_0 and B_0 are the dominant components. This anomalous behavior has been experimentally observed. Although the microwave absorption lines in Fig. 3(a) move closer together if a constant electric field is turned on, they move apart if an rf field of about 16 megacycles is applied.

4.4 Discussion of Experimental Results

In Fig. 4, the theoretical and experimental results are compared. The solid curve is a plot of Eq. (55) while the circled points were obtained experimentally. ν_{ab} was set equal to 12.78 Mc in Eq. (55) because this is the value calculated from the frequencies of the microwave lines[12] when it is assumed in accordance with the theory of l-type doubling[10] that $\omega_{cd}=3\omega_{ab}$. The theory and experiment are seen to agree within the experimental uncertainty. The data seems to indicate that $\nu_{ab}=12.76$ Mc might be a better fit than $\nu_{ab}=12.78$ Mc, but this difference is not experimentally significant here.

The estimated maximum experimental error which is indicated by the vertical lines on the figure increases with the field strength for several reasons. One is that the components are separated by a greater frequency when the field is stronger; the greater the separation between the components the more likely it is that spurious intensity differences will be introduced by reflections in the waveguide or by variations of the power output of the klystron with frequency. In addition the intensities of the components vary more rapidly with rf frequency when the field strength is small. A given uncertainty in determining the intensities of the components thus results in a smaller frequency uncertainty for a weak rf field than for a strong one. Let R be the minimum detectable fractional difference in intensity of the two components. It follows from Eq. (30) that

$$|\omega_{ab}-\omega_0| = (R/2)\gamma.$$

For a given R, the error in $|\omega_{ab}-\omega_0|$ is thus proportional to the "splitting," γ. For example, if the components can be made equal to within 4% $R=0.04$ and if the "splitting" is one Mc, the uncertainty in ω_0 is about 0.02 Mc. This is approximately the uncertainty is measuring microwave frequencies when the line width is of the order of $\frac{1}{2}$ Mc. If the line width could be reduced, a weaker rf field could be used, thus reducing the "splitting" and increasing the resolution.

To summarize: resonant modulation provides a method of measuring the energy difference between two energy levels. The precision is approximately equal to that with which the microwave absorption line can be located. However, if it is possible to measure accurately the voltage applied to the wave guide, the energy separation between closely spaced levels can be obtained by making frequency measurements in the rf rather than the microwave region. In addition, under some conditions data could be obtained by resonant modulation which could not be obtained by other techniques. For example, in Fig. 3(a), if there were no observable microwave transition from b to d, or the relationship between ω_{ab} and ω_{cd} were not known, one could not measure ω_{ab}. Using resonant modulation, however, it is possible to determine ω_{ab} by observing a single microwave absorption line.

4.5 Details of the Experimental Apparatus and Procedure

Figure 5 is a schematic diagram of the experimental arrangement used. The apparatus outside the dashed area is a conventional Stark-modulation microwave spectroscope. The apparatus inside the area was added for this experiment. It consists simply of an oscillator, a vacuum-tube voltmeter, and a circuit for tuning out the capacitance of the wave guide.

The oscillator is a standard Hartley circuit using an 829 tube and having a number of plug-in coils so it can oscillate in the 11–14 Mc region near ν_{ab} and also the 35-45 Mc region near ν_{cd}.

The vacuum-tube voltmeter used was a General Radio type 1800A which is claimed to be accurate for frequencies much higher than any used in this experiment.

The tuning circuit was used to increase the impedance presented to the oscillator by the capacitance between the wave guide and septum. This is about 1000 $\mu\mu$f which represents a reactance of about 12 ohms at 13 Mc and 4 ohms at 39 Mc. If 10 volts were maintained

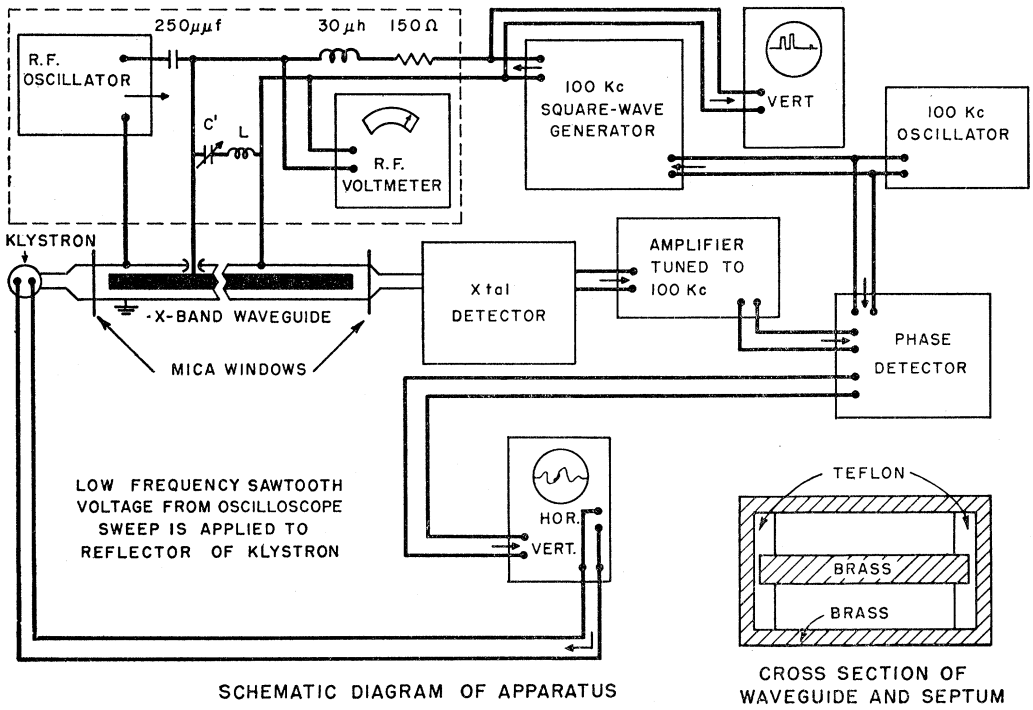

FIG. 5. Schematic diagram of experimental apparatus.

across the septum, rf currents of about 0.83 and 2.50 amperes would be drawn, requiring a sizable oscillator. Instead, in the 13 Mc region this wave-guide capacitance, C, is resonated with a circuit consisting of an inductance and a small variable capacitance in series. These are L and C' in Fig. 5.

The effective capacitance across the coil is the series combination of C and C' which is about equal to C' if $C' \ll C$. The product LC' is adjusted to resonate with the oscillator frequency, thus increasing the impedance of the oscillator's load by a factor equal to the Q of the resonant circuit.

The wave guide is about 1 meter long and is fed near its center. Its effective length of 0.5 meter is thus considerably less than a quarter-wavelength even at 39 Mc so the rf field strength is fairly uniform along its length. The design of the septum, as shown in Fig. 5, is such that the field is also quite uniform over the cross section of the guide.

The 250 $\mu\mu$f condenser isolates the rf oscillator at low frequencies and prevents the output coil of the oscillator from short-circuiting the square-wave generator. Similarly, the 30 μh inductance keeps the square-wave generator from loading the circuit at 13 or 39 Mc. The 150 ohm resistor critically damps the resonant circuit formed by this inductance and the wave-guide capacitance.

The microwave frequency standard used has been described before.[14]

[14] See for example: S. Geschwind, Ann. N. Y. Acad. Sci. **55**, 751 (1952).

ACKNOWLEDGMENTS

The authors are very grateful for help from Mr. George C. Dousmanis, who carried out the numerical calculations reported here, and from Miss Carlotta Heller who assisted with preparation of the manuscript. We would also like to thank the many members of the Columbia Radiation Laboratory who contributed to the construction and maintenance of the experimental apparatus.

APPENDIX 3.1a. PROOF OF EQS. (10)

In Eq. (8) assume that if k and l are greater than some integer j, A_k and B_l are sufficiently small to be neglected. Assuming j is odd and positive

$$\left[L_a+\frac{\omega_{ab}}{\beta_{ab}}\mp j\frac{\omega}{\beta_{ab}}\right]B_{\pm j}=-A_{\pm(j-1)},$$

$$\left[L_a\mp(j-1)\frac{\omega}{\beta_{ab}}\right]A_{\pm(j-1)}=B_{\pm(j-2)}-B_{\pm j}$$

$$=-B_{\pm(j-2)}+\frac{A_{\pm(j-1)}}{L_a+\dfrac{\omega_{ab}}{\beta_{ab}}\mp j\dfrac{\omega}{\beta_{ab}}},$$

$$\left[L_a\mp\frac{(j-1)\omega}{\beta_{ab}}-\frac{1}{L_a+\dfrac{\omega_{ab}}{\beta_{ab}}\mp j\dfrac{\omega}{\beta_{ab}}}\right]A_{\pm(j-1)}=B_{\pm(j-2)}. \quad (2a)$$

Now continue in the same manner

$$\left[L_a+\frac{\omega_{ab}}{\beta_{ab}}\mp(j-2)\frac{\omega}{\beta_{ab}}\right]B_{\pm(j-2)}=-A_{\pm(j-3)}-A_{\pm(j-1)}. \tag{3a}$$

Substitute Eq. (2a) into (3a)

$$\left[L_a+\frac{\omega_{ab}}{\beta_{ab}}\mp(j-2)\frac{\omega}{\beta_{ab}}-\cfrac{1}{L_a\mp(j-1)\frac{\omega}{\beta_{ab}}-\cfrac{1}{L_a+\frac{\omega_{ab}}{\beta_{ab}}\mp\frac{j\omega}{\beta_{ab}}}}\right]=A_{\pm(j-3)}.$$

Continuing this procedure, we can generalize to

$$\frac{B_{\pm(j-m)}}{A_{\pm(j-m-1)}}=\cfrac{1}{L_a+\frac{\omega_{ab}}{\beta_{ab}}\mp(j-m)\frac{\omega}{\beta_{ab}}-\cfrac{1}{L_a\mp(j-m+1)\frac{\omega}{\beta_{ab}}-\cdots\cfrac{-1}{L_a+\frac{\omega_{ab}}{\beta_{ab}}\mp\frac{j\omega}{\beta_{ab}}}}},$$

$$\frac{A_{\pm(j-n)}}{B_{\pm(j-n-1)}}=\cfrac{1}{L_a\mp(j-n)\frac{\omega}{\beta_{ab}}-\cfrac{1}{L_a+\frac{\omega_{ab}}{\beta_{ab}}\mp(j-n+1)\frac{\omega}{\beta_{ab}}-\cdots-\cfrac{1}{L_a\mp\frac{j\omega}{\beta_{ab}}}}},$$

where m is any positive even integer and n any positive odd integer. Now let $j-m=l$ and $j-n=k$, and let $j\to\infty$ while holding k and l constant. Then the above approaches Eq. (10).

APPENDIX 3.1b. EVALUATION OF EQ. (11) WHEN $\omega=0$

When $\omega=0$ Eq. (11) becomes

$$\frac{L_a}{2}=\cfrac{1}{L_a+\frac{\omega_{ab}}{\beta_{ab}}-\cfrac{1}{L_a-\cfrac{1}{L_a+\frac{\omega_{ab}}{\beta_{ab}}-\cdots}}}.$$

Since this continued fraction repeats indefinitely, eliminating a finite number of terms does not change its value, and the above equation can be written

$$\frac{L_a}{2}=\cfrac{1}{L_a+\frac{\omega_{ab}}{\beta_{ab}}-\cfrac{1}{L_a-\frac{L_a}{2}}}.$$

This is equivalent to the quadratic equation

$$L_a^2+\frac{\omega_{ab}}{\beta_{ab}}L_a+4=0,$$

whose solution is

$$L_c=-\frac{\omega_{ab}}{2\beta_{ab}}\pm\left[\left(\frac{\omega_{ab}}{2\beta_{ab}}\right)^2+4\right]^{\frac{1}{2}}.$$

This is the same result which can be obtained by direct diagonalization of the time-independent Schrödinger equation.

APPENDIX 3.1c. DERIVATION OF OTHER SOLUTIONS OF EQ. (8)

Assume that L_a' and B_l', $\cdots A_k'\cdots$ satisfy Eq. (8) and that they are related to another set of quantities L_a, $B_l\cdots$, $A_k\cdots$ by

$$L_a'=L_a-\frac{\omega_{ab}-\omega}{\beta_{ab}},\quad B_l'=A_{1-l},\quad A_k'=-B_{1-k}. \tag{12}$$

Since the primed quantities are assumed to satisfy (8)

$$\left[L_a'-\frac{k\omega}{\beta_{ab}}\right]A_k'=-B_{k-1}'-B_{k+1}',$$

$$\left[L_a'+\frac{\omega_{ab}}{\beta_{ab}}-l\omega\right]B_l'=-A_{l+1}'-A_{l+1}'.$$

Now substitute the unprimed quantities to determine what equations they must obey.

$$\left[L_a+\frac{\omega_{ab}}{\beta_{ab}}+\frac{(k-1)\omega}{\beta_{ab}}\right]B_{1-k}=-A_{1-k+1}-A_{1-k-1},$$

$$\left[K_a+\frac{(l-1)\omega}{\beta_{ab}}\right]A_{1-l}=-B_{1-l+1}-B_{1-l-1}.$$

Taking the complex conjugate of these equations, and rewriting by letting $l'=1-k$ and $k'=1-l$, we have:

$$\left[L_a-\frac{k'\omega}{\beta_{ab}}\right]A_{k'}=-B_{k'-1}-B_{k'+1},$$

$$\left[L_a+\frac{\omega_{ab}}{\beta_{ab}}-\frac{l'\omega}{\beta_{ab}}\right]B_{l'}=-A_{l'-1}-A_{l'+1}.$$

These equations have the same form as (8) so we have shown that the primed quantities in (12) define a new solution of (8), provided that the unprimed quantities from which they are derived form a solution.

In a similar manner, it can be shown that from each of these solutions can be derived an infinite number of other solutions, of (8), which are given in Eq. (14).

Deriving Solutions of Eq. (9) from those of (8)

Rewrite (9),

$$\left[L_b-\frac{\omega_{ab}}{\beta_{ab}}-\frac{l\omega}{\beta_{ab}}\right]=-\frac{B_{l-1}}{B_0}-\frac{B_{l+1}}{B_0},$$

$$\left[L_b-\frac{k\omega}{\beta_{ab}}\right]=-\frac{A_{k-1}}{B_0}-\frac{A_{k+1}}{B_0}.$$

Now assume L_b, $A_l/A_0\cdots$, $B_k/B_0\cdots$, satisfy this equation and are related to the quantities L_a, $A_k/A_0\cdots$, $B_l/A_0\cdots$, by Eq. (15).

Then substituting for L_b, $\cdots$ above, one obtains

$$\left[L_a+\frac{\omega_{ab}}{\beta_{ab}}+\frac{l\omega}{\beta_{ab}}\right]\frac{B_{-l}}{A_0}=-\frac{A_{-l+1}}{A_0}-\frac{A_{-l-1}}{A_0},$$

$$\left[L_a+\frac{k\omega}{\beta_{ab}}\right]\frac{A_{-k}}{A_0}=-\frac{B_{-k+1}}{A_0}-\frac{B_{-k-1}}{A_0},$$

which is (8) again. Thus we have proved that the new set of quantities defined in Eq. (15) is a solution of (9) if L_a, $A_k/A_0\cdots$, $B_0/A_0\cdots$ satisfy (8).

APPENDIX 3.3a. SOLUTION OF EQ. (37) TO SECOND ORDER

Equation (37) can be written as

$$L_a=\frac{1}{L_a+\dfrac{\omega_{ab}-\omega}{\beta_{ab}}+\dfrac{\beta_{ab}}{2\omega}+\dfrac{\beta_{ab}^2}{4\omega_{ab}^2}L_a}+\frac{\beta_{ab}}{\omega_{ab}+\omega}.$$

Now clear of fractions and make use of the relations

$$\frac{1}{\omega}=\frac{1}{\omega_{ab}}+\frac{\omega_{ab}-\omega}{\omega_{ab}^2}+\cdots$$

$$\frac{1}{\omega_{ab}+\omega}=\frac{1}{2\omega_{ab}}+\frac{\omega_{ab}-\omega}{4\omega_{ab}^2}+\cdots$$

neglecting terms which are small when $(\omega_{ab}-\omega)/\omega_{ab}\ll 1$. We then have

$$L_a^2\left[1+\frac{\beta_{ab}}{2\omega_{ab}^2}\right]+\frac{\omega_{ab}-\omega}{\beta_{ab}}L_a=1+\frac{\omega_{ab}-\omega}{\omega_{ab}+\omega}+\frac{\beta_{ab}^2}{4\omega_{ab}^2}.$$

This quadratic equation has the solutions:

$$L_a=-\frac{\omega_{ab}-\omega}{2\beta_{ab}}+\frac{\beta_{ab}^2}{4\omega_{ab}^2}\frac{\omega_{ab}-\omega}{\beta_{ab}}\pm\frac{y}{2}\left[1-\frac{\beta_{ab}^2}{2y^2\omega_{ab}^2}\left(1+\frac{(\omega_{ab}-\omega)^2}{\beta_{ab}^2}\right)\right]^{\frac{1}{2}},$$

where

$$y=+\left[\frac{(\omega_{ab}-\omega)^2}{\beta_{ab}^2}+\frac{8\omega_{ab}}{\omega_{ab}+\omega}\right]^{\frac{1}{2}}.$$

After expanding the square root, this can be written:

$$L_a=\rho_\pm+\frac{\beta_{ab}^2}{4\omega_{ab}^2}\left[\frac{\omega_{ab}-\omega}{\beta_{ab}}\mp\frac{1}{y}\mp\frac{(\omega_{ab}-\omega)^2}{\beta_{ab}^2 y}\right],$$

where $\rho_\pm$ are our previous solutions for L_a, as given by Eq. (33). The upper signs are to be used when $\omega<\omega_{ab}$ and the lower signs when $\omega\geqslant\omega_{ab}$.

Substitute for y in this equation:

$$L_a=\rho_\pm\left[1-\frac{\beta_{ab}^2}{4\omega_{ab}^2}\frac{1-2\dfrac{\omega_{ab}-\omega}{\beta_{ab}}\rho_\pm}{2(\rho_\pm)^2+\dfrac{\omega_{ab}-\omega}{\beta_{ab}}\rho_\pm}\right].$$

Remembering that ρ satisfies Eq. (32) and substituting for $[(\omega_{ab}-\omega)/\beta_{ab}]\rho$, one obtains Eq. (38). In this step the terms $(\omega_{ab}-\omega)/(\omega_{ab}+\omega)(\beta_{ab}^2/4\omega_{ab}^2)\rho$ are neglected for they are always of higher than second order.

The correction term in (38) should be omitted when $2\rho^2-1$ becomes negative, for then its contribution becomes comparable to third-order terms which have already been omitted.

APPENDIX 3.4a. AMPLITUDE COEFFICIENTS NEAR RESONANCE

The other amplitude coefficients in the resonant region are:

$$\frac{B_{-1}}{A_0}=-\frac{A_{+1}}{B_0}=\frac{-1}{L_a+(\omega_{ab}+\omega)/\beta_{ab}+\cdots}$$

$$=-\left[\frac{\beta_{ab}}{\omega_{ab}+\omega}-\frac{\beta_{ab}^2}{(\omega_{ab}+\omega)^2}L_a+\cdots\right].$$

Using the approximation for $\beta_{ab}/(\omega_{ab}+\omega)$ again leads to Eq. (43). Similarly:

$$\frac{A_{+2}}{A_0}=\frac{B_{-2}}{B_0}=\frac{-1}{L_a-2\omega/\beta_{ab}}\frac{B_{+1}}{A_0}=\frac{B_{+1}}{A_0}\left[\frac{\beta_{ab}}{2\omega}+\frac{\beta_{ab}^2}{4\omega^2}\rho\right],$$

$$\frac{A_{+2}}{A_0}=\frac{B_{+1}}{A_0}\left[\frac{\beta_{ab}}{2\omega_{ab}}+\frac{\beta_{ab}^2}{4\psi_{ab}^2}\left(\frac{2(\omega_{ab}-\omega)}{\beta_{ab}}+\rho\right)\right].$$

APPENDIX 4.2a. CALCULATION OF $(B_{+1})/A_0$ TO SECOND ORDER NEAR RESONANCE

We wish to employ Eq. (41) and obtain a more explicit solution for B_{+1}/A_0. First β_{ab}/K_{ab} must be calculated. Use Eq. (40) and expand the radical. Then, for $\omega \gtrless \omega_{ab}$

$$\frac{K_{ab}}{\beta_{ab}}=-1+\frac{\omega_{ab}-\omega}{2\beta_{ab}}-\frac{(\omega_{ab}-\omega)^2}{8\beta_{ab}^2}-\frac{\omega_{ab}-\omega}{2(\omega_{ab}+\omega)}.$$

By taking the reciprocal of this equation, one obtains:

$$\frac{\beta_{ab}}{K_{ab}}=-\left[1+\frac{\omega_{ab}-\omega}{2\beta_{ab}}+\frac{(\omega_{ab}-\omega)^2}{8\beta_{ab}^2}-\frac{\omega_{ab}+\omega}{4\omega_{ab}}\right].$$

Use this expression in Eq. (41) and also make use of the fact that $(2\rho^2-1)/(\rho^2+1)\approx\frac{1}{2}$ very near resonance. Then Eq. (50) follows.

Calculation of ω_0 to Second Order

Substitute Eqs. (50) and (51) into (49):

$$1+\frac{\beta_{ab}}{2\omega_{ab}}+\frac{\beta_{ab}^2}{8\omega_{ab}^2}+\frac{\beta_{cd}}{\omega_{cd}-\omega_{ab}}+\frac{\beta_{ab}\beta_{cd}}{2\omega_{ab}(\omega_{cd}-\omega_{ab})}+\frac{\beta_{ab}^2}{4\omega_{ab}^2}$$
$$+\frac{\beta_{ab}\beta_{cd}}{2\omega_{ab}(\omega_{cd}-\omega_{ab})}+\frac{\omega_{ab}-\omega_0}{\beta_{ab}}\left[\frac{1}{2}+\frac{\beta_{ab}}{4\omega_{ab}}\right.$$
$$\left.+\frac{\beta_{cd}}{2(\omega_{cd}-\omega_{ab})}\right]+\frac{(\omega_{ab}-\omega_0)^2}{8\beta_{ab}^2}$$
$$=1-\frac{\beta_{cd}}{\omega_{cd}-\omega_{ab}}-\frac{\beta_{ab}^2}{4\omega_{ab}^2}-\frac{\beta_{ab}\beta_{cd}}{2\omega_{ab}(\omega_{cd}-\omega_{ab})}+\frac{\beta_{ab}\beta_{cd}}{2\omega_{ab}(\omega_{cd}-\omega_{ab})}.$$

This simplifies to:

$$\frac{X^2}{8}+X\left[\frac{1}{2}+\frac{\beta_{ab}}{4\omega_{ab}}+\frac{\beta_{cd}}{2(\omega_{cd}-\omega_{ab})}\right]$$
$$=-\frac{\beta_{ab}}{2\omega_{ab}}-\frac{2\beta_{cd}}{\omega_{cd}-\omega_{ab}}-\frac{5}{8}\frac{\beta_{ab}^2}{\omega_{ab}^2}-\frac{3}{4}\frac{\beta_{ab}\beta_{cd}}{\omega_{ab}(\omega_{cd}+\omega_{ab})},$$

where

$$X=\frac{\omega_{ab}-\omega_0}{\beta_{ab}}.$$

By ignoring the X^2 term temporarily, one obtains:

$$X'=-\frac{\beta_{ab}}{\omega_{ab}}-\frac{4\beta_{cd}}{\omega_{cd}-\omega_{ab}}-\frac{3}{4}\frac{\beta_{ab}^2}{\omega_{ab}^2}+\frac{4\beta_{cd}^2}{(\omega_{cd}-\omega_{ab})^2}.$$

To second order:

$$(X')^2=\frac{\beta_{ab}^2}{\omega_{ab}^2}+\frac{16\beta_{cd}^2}{(\omega_{cd}-\omega_{ab})^2}+\frac{8\beta_{ab}\beta_{cd}}{\omega_{ab}(\omega_{cd}-\omega_{ab})}.$$

Now subtract $(X')^2/2$ from X',

$$X=-\frac{\beta_{ab}}{\omega_{ab}}-\frac{4\beta_{cd}}{\omega_{cd}-\omega_{ab}}-\frac{\beta_{ab}^2}{\omega_{ab}^2}-\frac{2\beta_{ab}\beta_{cd}}{\omega_{ab}(\omega_{cd}-\omega_{ab})},$$

from which Eq. (52) follows.